INFORMATION TO USERS

This reproduction was made from a copy of a document sent to us for microfilming. While the most advanced technology has been used to photograph and reproduce this document, the quality of the reproduction is heavily dependent upon the quality of the material submitted.

The following explanation of techniques is provided to help clarify markings or notations which may appear on this reproduction.

1. The sign or "target" for pages apparently lacking from the document photographed is "Missing Page(s)". If it was possible to obtain the missing page(s) or section, they are spliced into the film along with adjacent pages. This may have necessitated cutting through an image and duplicating adjacent pages to assure complete continuity.

2. When an image on the film is obliterated with a round black mark, it is an indication of either blurred copy because of movement during exposure, duplicate copy, or copyrighted materials that should not have been filmed. For blurred pages, a good image of the page can be found in the adjacent frame. If copyrighted materials were deleted, a target note will appear listing the pages in the adjacent frame.

3. When a map, drawing or chart, etc., is part of the material being photographed, a definite method of "sectioning" the material has been followed. It is customary to begin filming at the upper left hand corner of a large sheet and to continue from left to right in equal sections with small overlaps. If necessary, sectioning is continued again—beginning below the first row and continuing on until complete.

4. For illustrations that cannot be satisfactorily reproduced by xerographic means, photographic prints can be purchased at additional cost and inserted into your xerographic copy. These prints are available upon request from the Dissertations Customer Services Department.

5. Some pages in any document may have indistinct print. In all cases the best available copy has been filmed.

University Microfilms International

300 N. Zeeb Road
Ann Arbor, MI 48106

Reproduced with permission of the copyright owner. Further reproduction prohibited without permission.

Reproduced with permission of the copyright owner. Further reproduction prohibited without permission.

1323279

WU-MING, CHANG

INFLUENCE OF WASHABILITY ON DISTRIBUTION OF MACERALS, MINERAL MATTER, MAJOR OXIDES AND TRACE ELEMENTS OF CERTAIN ALASKAN COAL

UNIVERSITY OF ALASKA M.SC. 1983

University Microfilms International 300 N. Zeeb Road, Ann Arbor, MI 48106

Reproduced with permission of the copyright owner. Further reproduction prohibited without permission.

Reproduced with permission of the copyright owner. Further reproduction prohibited without permission.

PLEASE NOTE:

In all cases this material has been filmed in the best possible way from the available copy. Problems encountered with this document have been identified here with a check mark __√__.

1. Glossy photographs or pages _____
2. Colored illustrations, paper or print _____
3. Photographs with dark background _____
4. Illustrations are poor copy _____
5. Pages with black marks, not original copy _____
6. Print shows through as there is text on both sides of page _____
7. Indistinct, broken or small print on several pages ✓
8. Print exceeds margin requirements _____
9. Tightly bound copy with print lost in spine _____
10. Computer printout pages with indistinct print _____
11. Page(s) _____ lacking when material received, and not available from school or author.
12. Page(s) _____ seem to be missing in numbering only as text follows.
13. Two pages numbered _____. Text follows.
14. Curling and wrinkled pages _____
15. Other _____

University
Microfilms
International

Reproduced with permission of the copyright owner. Further reproduction prohibited without permission.

Reproduced with permission of the copyright owner. Further reproduction prohibited without permission.

INFLUENCE OF WASHABILITY ON DISTRIBUTION OF MACERALS, MINERAL MATTER, MAJOR OXIDES AND TRACE ELEMENTS OF CERTAIN ALASKAN COAL

A

THESIS

Presented to the Faculty of the University of Alaska

in Partial Fulfillment of the Requirements

for the Degree of

MASTER OF SCIENCE

BY

CHANG WU-MING, B.S.

Fairbanks,Alaska

December 1983

Reproduced with permission of the copyright owner. Further reproduction prohibited without permission.

INFLUENCE OF WASHABILITY ON DISTRIBUTION OF MACERALS, MINERAL MATTERS, MAJOR OXIDES AND TRACE ELEMENTS OF CERTAIN ALASKAN COAL

RECOMMENDED:

Ernest N. Wolff

David R. Maxwell

Earl A. Beistline

Chairman, Advisory Committee

Frank J. Szudzyk

Department Head

APPROVED: William S. Reckmeyer for

Vice Chancellor for Research and Advanced Study

24 Oct 83

Date

Reproduced with permission of the copyright owner. Further reproduction prohibited without permission.

ABSTRACT

Various aspects of influence of washability have been examined by employing six Alaskan coal samples. Of major concern are the effects of washability on the distribution of macerals groups and microlithotypes, concentration of minerals in the densimetric fractions, liberation and separation of minerals, concentration of chemical constituents of ash in the densimetric fractions, and the fusibility of ash of each densimetric fractions.

The results show that characteristics of densimetric fractions exhibit certain trends which are related to specific gravity of separation and particle size. Although the coals studied showed trends of their own, certain characteristics such as ash composition and ash fusibility were rank dependent. Both the $K(SiO_2/\ Al_2O_3)$ ratio and major oxides (SiO_2, Al_2O_3, Fe_2O_3, MgO, and CaO) gave statistically significant correlations to give good predictions of Initial Deformations Temperature of ash.

Reproduced with permission of the copyright owner. Further reproduction prohibited without permission.

TABLE OF CONTENTS

Reproduced with permission of the copyright owner. Further reproduction prohibited without permission.

Reproduced with permission of the copyright owner. Further reproduction prohibited without permission.

Reproduced with permission of the copyright owner. Further reproduction prohibited without permission.

LIST OF FIGURES

Reproduced with permission of the copyright owner. Further reproduction prohibited without permission.

Reproduced with permission of the copyright owner. Further reproduction prohibited without permission.

LIST OF TABLES

Reproduced with permission of the copyright owner. Further reproduction prohibited without permission.

Reproduced with permission of the copyright owner. Further reproduction prohibited without permission.

Reproduced with permission of the copyright owner. Further reproduction prohibited without permission.

Reproduced with permission of the copyright owner. Further reproduction prohibited without permission.

Reproduced with permission of the copyright owner. Further reproduction prohibited without permission.

Reproduced with permission of the copyright owner. Further reproduction prohibited without permission.

Reproduced with permission of the copyright owner. Further reproduction prohibited without permission.

ACKNOWLEDGEMENTS

I wish to express my deepest appreciation to my committee chairman, Dr. Pemmasani D. Rao, as well as the three other members of my committee, Dr. Ernest N. Wolff, Dr. Earl H. Beistline, and Dr. David R. Maneval, for their guidance and assistance during the course of this thesis.

I wish to extend my acknowledgements to Dr. Donald J. Cook, visiting associate director, Mineral Industry Research Laboratory and Dr. Hok S. Liu, director, graduate study program of Mineral and Material Engineering, National Cheng Kung University, for their encouragement. Research was funded by the U.S. Department of Energy, State of Alaska Special Appropriation and Coal Research, and the School of Mineral Industry and their financial assistance is gratefully acknowledged.

Thanks are also due to Jane E. Smith, Juliet Cruz, and other individuals for their cooperation and help to accomplish research presented in this report.

Reproduced with permission of the copyright owner. Further reproduction prohibited without permission.

CHAPTER 1

INTRODUCTION AND OBJECTIVES

Introduction

Alaska has abundant coal resources ranging in rank from subbituminous to anthracite and is capable of supplying needed energy for the west coast as well as Pacific rim nations. Washability studies provide basic data required for evaluating the behavior of each coal in processing. Physical and chemical characteristics of coal and its ash, the mineralogy and petrology of raw coal and of the washed products are also becoming major concerns in industrial utilization. Rao and Wolff (1979,1980,1982a&b) conducted washability studies of 50 coal seams from Alaska. Their evaluation of washability products was limited to ash, heating value, pyritic sulfur and total sulfur.

This study is intended to evaluate the quality of the washed product in terms of ash composition, ash fusibility, petrology and mineral matter distribution. Six samples were selected, one from each of the major coal fields. The seams selected are from a currently or formerly operating coal mine or from a deposit that has a potential to be mined in the foreseeable future.

Reproduced with permission of the copyright owner. Further reproduction prohibited without permission.

These are:

1) Northern Alaska coal field---Cape Beaufort, No. 7 bed,

2) Nenana coal field---Usibelli coal mine, No. 3 seam,

3) Matanuska coal field---Site of former Evan Jones coal mine No. 5 bed,

4) Yentna coal field---Johnson creek, (Mobil oil Co. Leases)

5) Beluga coal field---Possible site of future Lone Ridge mine, Green seam (Placer Amex Inc. Leases)

6) Chignik coal field---former Chignik river mine.

Each of those samples was examined through

A) mineralogical analyses of low temperature ash (LTA),

B) determination of major oxides and trace elements,

C) microscopic studies to determine the petrology of each washed product.

The methods for analyses include:

a) X-ray diffraction and infrared spectrometric analyses for determination of mineral in LTA,

b) X-ray fluorescence spectrometric determination of major oXides in coal ash,

c) inductively couple argon plasma analyses for trace elements,

d) maceral groups and microlithotypes by combined analysis,

Reproduced with permission of the copyright owner. Further reproduction prohibited without permission.

e) ash fusibility determinations providing examples of interactive influence of major oxides on the behavior of the ash of each washed coal product.

Objectives

The conventional washing processes for industrial utilization of coal, influence the quality of washed coal, which in turn determines the performance reliability and overall cost of the system.

The efficiency of a coal washing process is determined by particle size and specific gravity of separation which is governed by washability curves. The chosen particle size of coal determines the extent to which mineral matter and macerals are liberated.

The washability curves give information about the yield of product, the percent of ash in the product, and percent of near-gravity material which influences the choice of a separation mechanism, and in turn the choice of a separation process.

Determination of the chemical composition of ash of a particular fraction gives information on ash behavior in utilization.

Reproduced with permission of the copyright owner. Further reproduction prohibited without permission.

The objectives of this study are summarized as follows:

I) study liberation of macerals in each washing product as influenced by chosen particle sizes.

II) study liberation of mineral matter in each washing product as influenced by chosen particle sizes.

III) study distribution of major oxides in the ash of each washing product as governed by particle size.

IV) study distribution of trace elements in the ash of each washing product as governed by particle size.

Reproduced with permission of the copyright owner. Further reproduction prohibited without permission.

CHAPTER 2

LITERATURE REVIEW

The Influence of Coal Characteristics on Mode of Utilization

A) Carbonization

I) Importance of macerals

Coal is a heterogenous substance, due to diverse paleobotanical origins of the organic portion and the various geological and environmental factors that caused the accumulation of the inorganic constituents. Geological processes such as pressure and temperature determine the rank of coal. The paleobotanical components and the processes to which they are subjected determine the types of components called the macerals. These are distinguishable by an observation under the microscopic inspection. So, the texture and the association of macerals determine the type of coal, just as the texture and constituent minerals determine rock type. Since relative concentration of macerals or microlithotypes affect the utilization of coal, it is important to examine the liberation and distribution of macerals and their response to washing. This in turn, would influence the design of a washing process. Table2-1 and 2-2 adopted from the

Reproduced with permission of the copyright owner. Further reproduction prohibited without permission.

Table 2-1 Summary of the macerals of hard coals

Group maceral	Maceral	Submaceral*	Maceral variety*
Vitrinite	Telinite	Telinite 1	Cordaitotelinite
		Telinite 2	Fungotelinite
			Xylotelinite
		Telocollinite	Lepidophytotelinite
		Gelocollinite	Sigillariotelinite
	Collinite	Desmocollinite	
		Corpocollinite	
	Vitrodetrinite		
Exinite	Sporinite		Tenuisporinite
			Crassisporinite
			Microsporinite
			Macrosporinite
	Cutinite		
	Resinite		
	Alginite		*Pila*-Alginite
			Reinschia-Alginite
	Liptodetrinite		
Inertinite	Micrinite		
	Macrinite		
	Semifusinite		
	Fusinite	Pyrofusinite	
		Degradofusinite	
	Sclerotinite	Fungosclerotinite	Plectenchyminite
			Corposclerotinite
			Pseudocorposclerotinite
	Inertodetrinite		

* incomplete can be expanded as required.

(Stach, 1971,1975)

Reproduced with permission of the copyright owner. Further reproduction prohibited without permission.

Table 2-2 Maceral classification of brown coals and lignites

	Maceral Subgroup	Maceral	Maceral Type
huminite	humotelinite	textinite	
		ulminite	texto-ulminite eu-ulminite
	humodetrinite	attrinite densinite	
	humocollinite	gelinite	porigelinite levigelinite
		corpohuminite	phlobaphinite pseudo-phlobaphinite
liptinite		sporinite cutinite resinite suberinite alginite liptodetrinite chlorophyllinite bituminite	
inertinite		fusinite semifusinite macrinite sclerotinite inertodetrinite	

(Stach, 1971,1975)

Reproduced with permission of the copyright owner. Further reproduction prohibited without permission.

Handbook coal Petrology (Stach, 1971,1975) show maceral classification of hard coals and brown coals respectively. Table 2-3 gives a summary of the maceral groups and microlithotypes, and table 2-4 gives a correlation of the huminite macerals of bituminous coal (Stach,1982). Due to variations in physical properties between macerals, coal preparation processes can influence the distribution and concentration of macerals in various sizes and gravity fractions. It is therefore a necessary concern to determine the character of the macerals and their influence on various utilization systems. The study of the applications of coal petrology has reached a high level of sophistication in the field of carbonization and is routinely used by the steel industry.

II) Application of coal petrology in coking

Coals that form coke and are usable for the reduction of iron ores in the blast furnace, are referred to as coking coals. The coking power is defined by their plastic properties and Free Swelling index, which depend on rank of coal and maceral composition. The dilatometer test can show with sufficient accuracy whether a coal has a good coking power or not. However, these tests do not reveal the reasons for differences in coking power

Reproduced with permission of the copyright owner. Further reproduction prohibited without permission.

Table 2-3 Summary of the microlithotype
(after International Handbook of Coal Petrography 1971,1975)

Maceral composition (mineral-free)		Microlithotype	Maceral-group composition (mineral-free)	Microlithotype group
Monomaceral				
Co	> 95 %	(Collite)*	V > 95 %	Vitrite
T	> 95 %	(Telite)*		
VD	> 95 %			
S	> 95 %	Sporite		
Cu	> 95 %	(Cutite)*		
R	> 95 %	(Resite)*	E (L) > 95 %	Liptite
A	> 95 %	Algite		
LD	> 95 %			
Sf	> 95 %	Semifusite		
F	> 95 %	Fusite	I > 95 %	Inertite
Sc	> 95 %	(Sclerotite)*		
ID	> 95 %	Inertodetrite		
M	> 95 %	(Macroite)*		
Bimaceral				
V + S	> 95 %	Sporoclarite		
V + Cu	> 95 %	Cuticoclarite	V + E (L) > 95 %	Clarite
V + R	> 95 %	(Resinoclarite)*		V, E(L)
V + LD	> 95 %			
V + M	> 95 %			
V + Sf	> 95 %			
V + F	> 95 %		V + I > 95 %	Vitrinertite
V + Sc	> 95 %			V, I
V + ID	> 95 %			
I + S	> 95 %	Sporodurite		
I + Cu	> 95 %	(Cuticodurite)*		
I + R	> 95 %	(Resinodurite)*	I + E (L) > 95 %	Durite
I + LD	> 95 %			I, E(L)
Trimaceral				
V, I, E	> 5 %	Duroclarite	V > I, E (L)	Trimacerite
		Vitrinertoliptite	E > I, V	V, I, E(L)
		Clarodurite	I > V, E (L)	

* The terms in parentheses are not at present in use.

Reproduced with permission of the copyright owner. Further reproduction prohibited without permission.

Reproduced with permission of the copyright owner. Further reproduction prohibited without permission.

Table 2-4 Correlation of the huminite macerals of brown coals and lignites with the vitrinite macerals of bituminous coal

Brown Coal — Lignite					Bituminous Coal		
Maceral Group	Maceral Subgroup	Maceral	Maceral Type	Maceral Variety	Maceral Type	Maceral	Maceral Group
huminite	humotelinite	textinite		A (dark) B (light)			vitrinite
		ulminite	texto-ulminite	A (dark) B (light)	telinite 1	telinite	
			eu-ulminite	A (dark) B (light)	telinite 2		
	humodetrinite	attrinite densinite				vitrodetrinite	
	humocollinite	gelinite	levi-gelinite	detrogelinite telogelinite eugelinite	desmocollinite		
					telocollinite	collinite	
			porigelinite		gelocollinite		
		corpo-huminite	phlobaphinite pseudo-phlobaphinite		corpocollinite		

(Stach, 1982)

of different coal blends with the same yield of volatile matter. Microscopic study is necessary to provide the answer. (Brown, Tayler and Cook, 1964) In general, macerals in the coking coals are grouped as "reactive" if they fuse when heated to 800° F and "inert" when they do not fuse (Schapiro et al.,1961). It is the behavior of vitrinite during coking that allows a coal to be classified as reactive. The inertinite group of macerals do not fuse on heating and are thus termed inerts. Sporinite and cutinite when heated with vitrinite act as softeners and cause the fluidity of vitrinite to increase. Pseudovitrinite is inferior to vitrinite in its coking properties and in certain extreme cases may behave in an entirely inert manner (Snyman, 1961). For low-volatile coals with reflectance greater than 1.4% R_o, the addition of any inerts is deleterious to coke strength, and strength decreases with increased inert content. However, for coals of medium and high volatile bituminous rank, the addition of 20-30% inerts strengthens the coke considerably. Isostability lines suggested by Schapiro and Gray (1964) have been widely applied. The procedure is applicable to a single coal or to a blend of two or more coals. Yet they indicate that prediction of coke strength is not entirely satisfactory with coals of high liptite content. Brown et al. (1964) Cook and Ed-

Reproduced with permission of the copyright owner. Further reproduction prohibited without permission.

wards (1970), and Cook and Wilson (1969) determined that the correlation of Shapiro and Gray is inapplicable to some Australian coals. Thompson and his associates (1974) concluded that coals can be separated into three populations based on the reflectance of vitrinite excluding pseudovitrinite (<0.7% R_o, 0.7% R_o-1.35% R_o, >1/35% R_o). Fig.2-1 show a discontinuous relationship between reflectance of reactive vitrinite and coke strength (tumbler stability). The discontinuity represents a fundamental change in vitrinite composition and should be relatable to specific stages in the coalification process. In practice, Fig.2-2 gives the effects of rank of coke from single coals. The strength of coke from blends of coals with less than 1.4% R_o can be predicted by calculating a weighted average of the stabilities for the individual coals using the curves shown in Fig.2-2a. When coals with greater than 1.4% R_o are added to the coals of lower reflectance, the strength of the coke from the blend is estimated by using Fig.2-3. The strength of the coke from the high and medium volatile coals (less than 1.4%) is estimated from Fig.2-2a and is plotted to the appropriate height above the zero abscissa point in Fig.2-3. Then the strength of the coke from the low volatile coals (greater than 1.4% R_o) is estimated from Fig.2-2b and is plotted above the 100% point in Fig.2-3. The coke strength of

Reproduced with permission of the copyright owner. Further reproduction prohibited without permission.

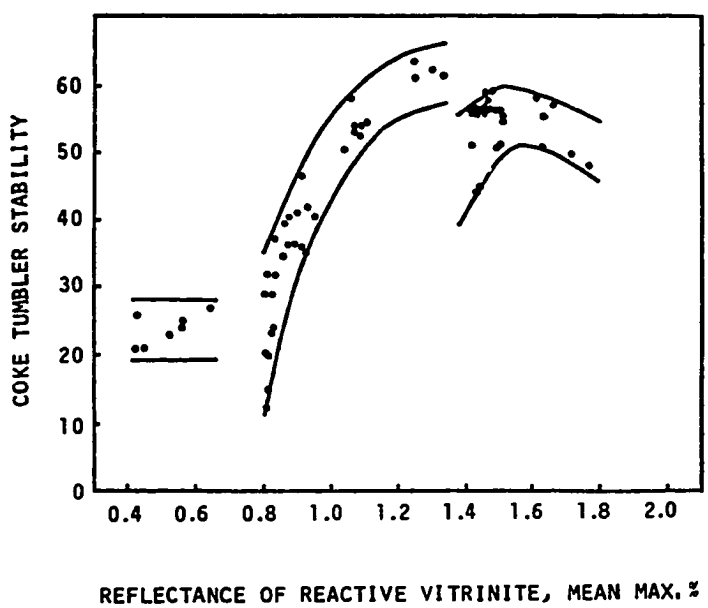

Figure 2-1 Discontinuous relationship between reflectance of reactive vitrinite and coke strength (Thompson,1974)

Reproduced with permission of the copyright owner. Further reproduction prohibited without permission.

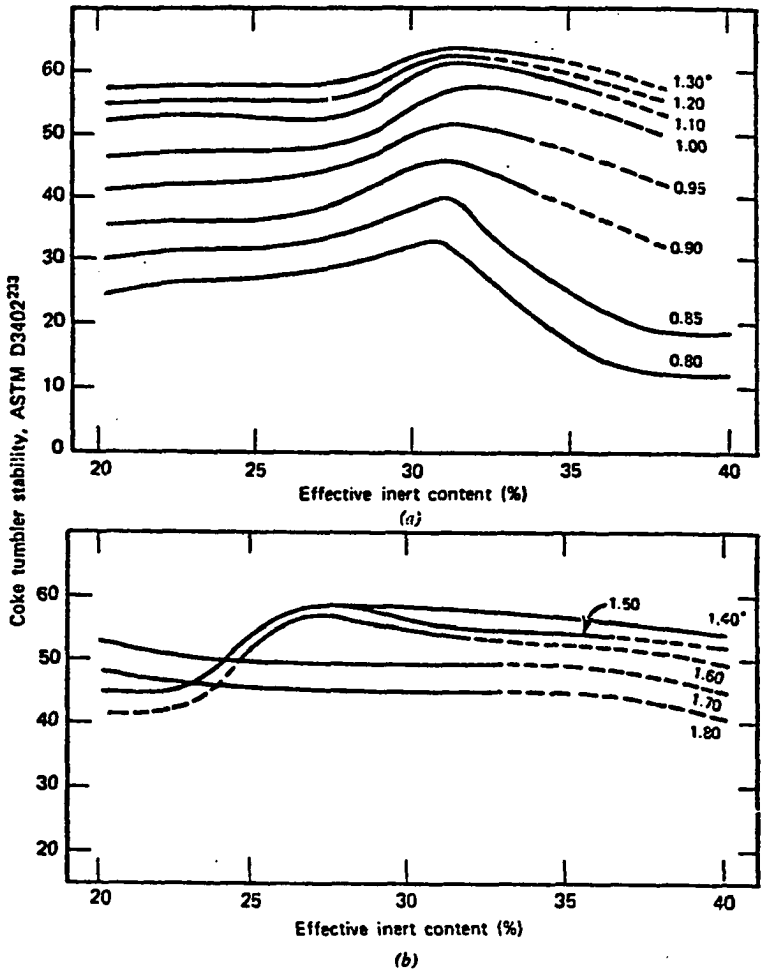

Figure 2-2 Effect of rank (vitrinite reflectance) and type (inert content) on stability of coke from single coals. Numbers with asterisks refer to reflectance of reactive vitrinite (mean max.%). (a) Curves for high and medium-volatile coals (1.4%). (b) Curves for low-volatile coals (1.4%). (Benedict et. al., 1968)

Reproduced with permission of the copyright owner. Further reproduction prohibited without permission.

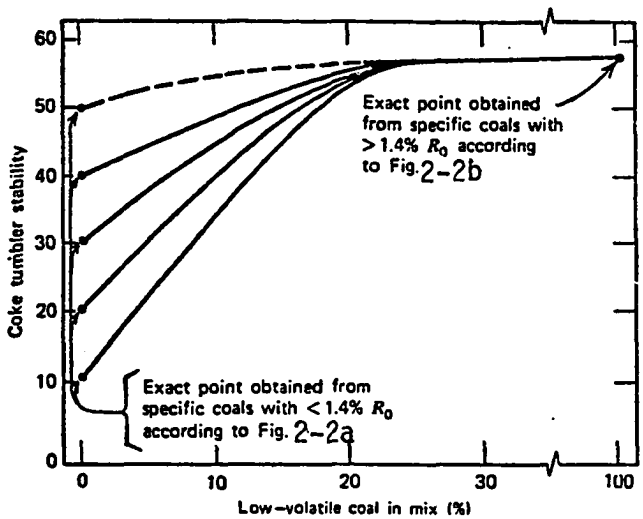

Figure 2-3 Combined correlation system for estimating coke strength from coal blend containing high and low-volatile coals.
(modified from Thompson, 1977)

Reproduced with permission of the copyright owner. Further reproduction prohibited without permission.

the blend is then estimated from this curve by employing the percentage of low volatile coal in the mix as the independent variable. In addition to coke stability, petrographic analyses have been used to predict contraction properties, coke oven pressures, and reactivity of the coke. Contraction increases with an increase in the concentraction of inerts in medium volatile coals (Schapiro, 1964). Coals with vitrinite reflectance above 1.35% can exert excessive pressure on oven walls during coking. A graphical correlation of vitrinite reflectance and oven pressure is given by Thompson and Benedict (1974). A highly reactive coke will be consumed too rapidly in a blast furnace. It, therefore, becomes necessary to evaluate the effect of coal properties on the reactivity of coke (Thompson,1970). Schapiro and Gray (1963) and Benedict Thompson (1973) correlated reactivity with coke structures assessed microscopically. Reactivity is principally related to coke porosity, which in turn is related to coal rank. Lower rank coals, alkalis, and inertinite macerals produce more highly reactive cokes.

III) The application of maceral group and microlithotype analyses

For reliable appraisal of a coking blend, analyses by maceral groups, microlithotypes or macerals have to be carried

Reproduced with permission of the copyright owner. Further reproduction prohibited without permission.

out in addition to the determination of rank and analyses by coal types. From table 2-5, the differences in the coking behavior of the three maceral groups is evident (Kroger, Kuthe & Gondermann, 1957). Exinite has the highest coking power compared to other maceral groups. However, exinite accounts for only 5% of the coal against 60 to 80% for vitrinite. The coking power of whole coal is therefore more controlled by vitrinite. (Kroger, Kuthe & Gondermann, 1957). Following the solution of the problem of determining the coking power of macerals or maceral groups as a function of rank, attempts have been make to predict or calculate the properties of high-temperature coke from the results of microscopic analyses. Brown, Taylor & Cook (1964) proposed an "index of petrographic composition" which combined vitrite and clarite. They believe that the sum of these two constituents gives a better indication of the proportion of reactives than the sum of vitrinite and exinite would. The maxium reflectance of vitrinite or the carbon content (dry ash free(daf)) of the coal sample is used as a measure of rank Fig. 2-4 shows three generalized diagrams. The rank index, on the ordinate, is plotted against the index of petrographic composition, on the abscissa. Fig. 2-4a shows the change of the BS swelling number as a function of rank and of the proportion of vitrite and

Reproduced with permission of the copyright owner. Further reproduction prohibited without permission.

Table 2-5 Dilation of the 3 maceral groups with increasing rank

Seam	V. M. (daf) %	Softening temperat. °C	Resolidification temperat. °C	Contraction Dilatation %		Coking power (see Table 31)
R						
V	36.13	396	459	30	— 27	1
I	22.54	—	—	3	—	1
E	68.77	(407)	—	(42)	(280)	5
Zollverein						
V	31.97	397	469	33	13	3
I	23.37	—	—	5	—	1
E	59.81	(419)	—	(48)	(430)	5
Anna						
V	28.36	401	487	23	110	4
I	19.18	—	—	3	—	1
E	37.08	(364)	488	42	(594)	5
Wilhelm						
V	23.50	410	484	22	107	4
I	16.98	—	—	8	—	1
E	22.57	413	483	23	44	3

* Kröger, Kuthe & Gondermann (1957).

Reproduced with permission of the copyright owner. Further reproduction prohibited without permission.

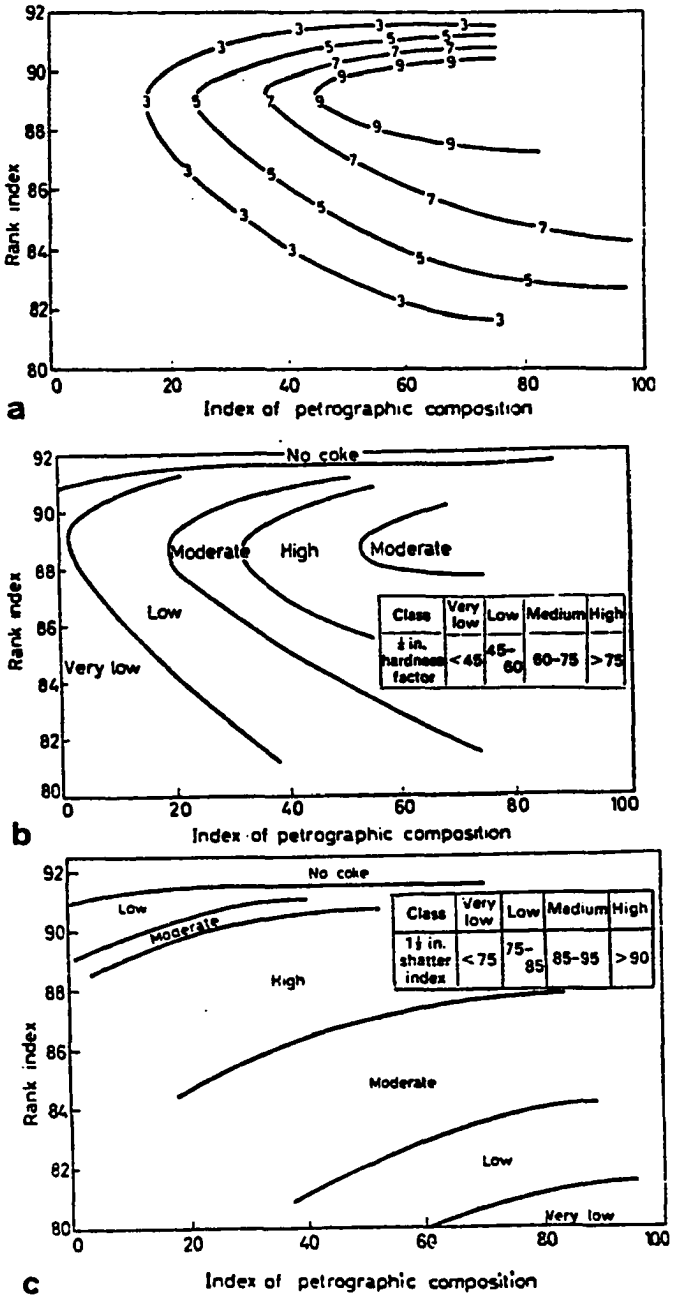

Figure 2-4 (a) Variation of B.S. swelling number with rank and petrographic composition (b) Variation of the 1/4 in. hardness factor with rank and petrography composition (c) Possible variation of shatter index with rank and petrographic composition. (Brown, et. al., 1964)

Reproduced with permission of the copyright owner. Further reproduction prohibited without permission.

clarite. In Fig. 2-4b the change in the strength of coke of high strength is represented graphically, using the same system of coordinates, and in Fig. 2-4c the corresponding results of the shatter test are shown. These diagrams are simple and clear, but they disregard the fact that coking coals which differ widely in their composition in terms of coal types can have the same carbon content. In addition the size consist and the rate of heating exert considerable influence on coke strength. Nevertheless, they supply rapid and in many cases sufficient preliminary information, especially when the examination is restricted to coal from one seam.

B) Effect of coal ash on combustion systems

The problems and possibilities related to the properties of coal ash will be addressed as follows.

I) origin of ash---inherent inorganic matter and extraneous inorganic matter.

II) chemical composition of the ash and of the reaction products formed during firing.

III) chemical constituents of ash that affect pertinent ash behavior during combustion---ash fusion. temperature, slag

Reproduced with permission of the copyright owner. Further reproduction prohibited without permission.

properties, fouling and corrosion.

I) Origin of ash in coal

The inorganic matter in coal originates from two sources: a) inorganic matter associated with original vegetal growth, contributes to what is generally called "inherent origin"
b) mineral matter that entered the coal seam from external sources during or after the period of coal formation is called "extraneous". Both of them account for 5% to 40% of the weight of coal. The conventional gravity separation methods can only reduce the amount of extraneous minerals. Large numbers of minerals have been identified in coal, the common extraneous minerals are listed below: (Nelson, 1953)
1)clay minerals---illite-sericite,montmonilonite,kaolinite,meta-halloysite
2)sulfides---pyrite,marcasite
3)carbonates---calcite,dolomite,ankerite,siderite
4)chlorides---halite,sylvite
5)other minerals---quartz,felspar,gypsum,apatite,magnetite,hematite,zircon,diaspore,garnet,hornblende

II) Chemical composition of ash

Reproduced with permission of the copyright owner. Further reproduction prohibited without permission.

A quantitative evaluation of mineral forms in coal is difficult. The composition of coal ash is customarily determined by chemical analyses of the residue produced by burning a sample of coal at a slow rate and at moderate temperature under oxidizing condition in a laboratory furnace. The ash thus formed is found to be comprised chiefly of compounds of silicon, aluminum, iron and calcium, with small amounts of magnesium, titanium, sodium and potassium. Although these elements are reported as oxides, they are actually present as silicates, oxides, sulfates, or other compounds, and may differ appreciably from the forms in which they originally occurred in coal, or the forms that might develop in an operating furnace.

Reid (1971) illustrated the progressive changes that can occur in coal minerals with rising temperature. Loss of water takes place first, followed by the evolution of CO_2 and SO_2 by a decomposition of carbonates and oxidation of pyrite. Sintering begins at about 1200° F, and liquid phases are formed that lead to melting and reaction between the ash particles to produce clinker and slag above 1800° F. Volatilization of Alkali compounds (Na_2O and K_2O) becomes appreciable as the temperature rises above 2000° F, Silica begins to volatilize at 2970° F under oxidizing conditions, and at a significant rate above 3780° F.

Reproduced with permission of the copyright owner. Further reproduction prohibited without permission.

It is evident that the only solids remaining above 3960° F would be CaO and Al_2O_3, and above 4860° F only Al_2O_3, in the case of coal ash containing 23% Fe_2O_3, 5% CaO+MgO and 2% Na_2O+K_2O under a neutral atmosphere.

III) Chemical constituents of coal ash as related to its behavior during combustion

1) Ash fusion temperature

The earliest investigations of ash behavior were concerned with evaluation of clinkering tendencies of different coals. ASTM, British and DIN standards each have their own currently applicable method. Although they differ in apparatus and measuring techniques, all are based on observing the temperature at which successive characteristic stages of fusion occur in a geometric form made of ash when heated in a laboratory furnace under specified conditions of atmosphere and rate of temperature rise. In the ASTM method, a sample of finely ground ash is pressed into a standard mold to form a triangular pyramid 3/4" high which is set vertically upon a cermic base within a gas fired or electrically heated furnace. The atmosphere is maintained in a mildly reducing condition or oxidizing condition by using a prepared gas. Temperatures are measured by an optical pyrometer

Reproduced with permission of the copyright owner. Further reproduction prohibited without permission.

or a thermocouple. The initial deformation temperature(I.D.T) is noted when the sharp apex or edges of the specimen first become rounded. Softening temperature is recorded when the specimen has deformed to approximately spherical shape, and fluid temperature(F.T) when the ash has become completely fused and has spread to a nearly flat liquid film upon the base. The softening temperature alone is frequently reported as the index of ash fusibility. It serves to indicate broad distinctions, but it is only partly descriptive of melting behavior. Since coal ash is a mixture rather than a compound with a well defined melting point, significance is attached to all reference temperatures and to the intervals between them, which vary appreciably for different ashes. The initial deformation temperature is broadly identified with the condition of surface stickiness, the softening temperature with plastic distortion or sluggish flow, and the fluid temperature with liquid mobility. These properties are not only related to the mechanics of clinker formation, but also the nature of clinker or slag produced. The so called "long" slags tend to develop tough dense formations; those of "short" fusion interval, which freeze abruptly, are more likely to form porous of friable structure. (Gumz,1956) With oxidizing condition in the test furnace, many ashes show higher values of fusion tem-

Reproduced with permission of the copyright owner. Further reproduction prohibited without permission.

perature than are observed in a reducing atmosphere. Although the reducing atmosphere provides a more dependable basis for standardization of test measurements and is regarded as characteristics of the fuel bed, oxidizing conditions in local areas or in other parts of the furnace may alter the behavior of the ash, independently of actual change in temperature.

2) Slag Properties

Slag tap furnaces for steam generation were widely installed during the 1930s to 1940s. They suffered from metal wastage of wall tubes. Fouling of surfaces between the slagging section and the economizer was troublesome because somewhere in the furnace or in the superheater and reheater sections, the molten droplets of slag carried by the flue gas had to freeze without adhering to heat transfer surfaces. For gasification, slagging operation appears highly attractive, both in fixed bed and entrained flow systems, so that interest in the properties of coal ash slag can be expected to increase.

The conventional measurement of fusion temperature gives a rough indication of ash behavior. Slag viscosity measurement become a more dependable guide with respect to liquid slag removal. Although widely different values of viscosity were ob-

Reproduced with permission of the copyright owner. Further reproduction prohibited without permission.

served, a consistent relationship among viscosity-temperature-composition has been noted. The studies emphasize the "silica percentage" concept of critical viscosity(Tcv) for the transition of a slag on cooling from a Newtonian fluid to a pseudoplastic solid. Other treatments of the influence of composition on the viscosity of coal ash slags have relied on the ratio of "bases" to "acids", or of $Fe_2O_3+CaO+MgO+Na_2O+K_2O/SiO_2+Al_2O_3+TiO_2$. (Sage,1960) Since the base/acid ratio and the silica percentage are closely related, it is possible to convert from one to the other. For practical purposes, the following relationships apply:

Silica percentage =92.33-66.67x(base/acid ratio)

base/acid ratio =1.385-0.015x(silica percentage)

This makes the conversion from one system to the other possible for those who prefer either the better accuracy and predictability based on the silica percentage or the simpler relationship of the base/ acid ratio. Fig. 2-5 illustrates the relationship between base/acid ratio of coal ash slags and the temperature where the viscosity is 250 poises, the maximum viscosity suitable for tapping slags from cyclone furnaces (Sage, 1960). A change in the state of oxidation of coal ash slags does not

Reproduced with permission of the copyright owner. Further reproduction prohibited without permission.

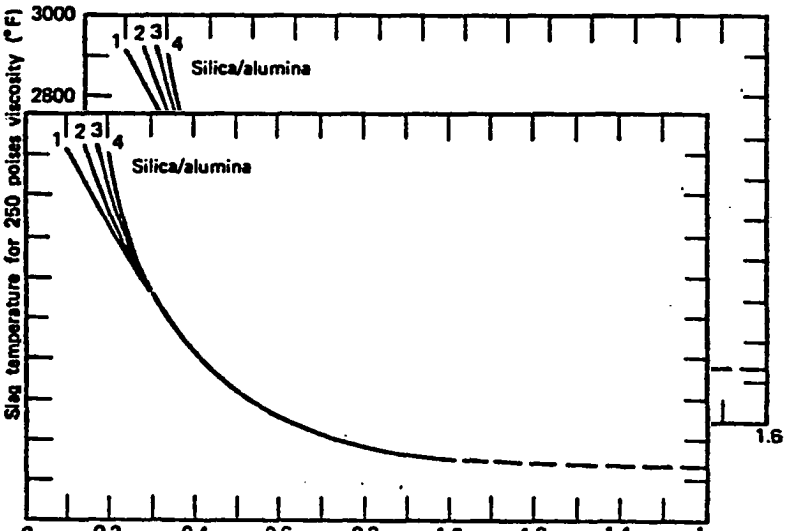

Figure [illegible] temperature for 250 poises viscosity at 20% ferric versus base-to acid ratio.
(Sage, 1960)

Reproduced with permission of the copyright owner. Further reproduction prohibited without permission.

substantially affect true Newtonian viscosity, but it does have a pronounced effect on Tcv. Since only the equivalent Fe_2O_3 in the slag responds to oxidizing or reducing conditions, the change in Tcv is greater with high iron slags than with low iron slags. Watt and Fereday (1969) conducted an intensive study of slag composition and viscosity. The correlation between the viscosity and the composition of coal ash slag, fully melted with no solid phases present , is represented by:

$m=.00835SiO2+.00601Al2O3-.109$

$c=.0415SiO_2+.0192Al_2O_3+.0276Fe_2O_3+.016CaO-3.92$

$\log \text{viscosity}=10^7 m/(t-150)^2+c$

where t is in degrees Celsius, and the analyses are expressed on the basis of : $SiO_2+Al_2O_3+Fe_2O_3+CaO+MgO=100$

with Fe_2O_3 being the total equivalent Fe_2O_3, given by analyses of the slag for forms of iron. Statistical evaluation shows that no significant error results from excluding Na_2O,K_2O,TiO_2 and S from this relationship. Hoy et al. (1965) also gave another simple relationship called the "S^2 correlation" $\log \text{viscosity}=4.468(S/100)^2+1.265\times10^4/T-7.44$

where S is the silica ratio 100 x $SiO_2/(SiO_2 + Fe_2O_3 + CaO +$

Reproduced with permission of the copyright owner. Further reproduction prohibited without permission.

MgO), and T is temperature (K). This simplest correlation was that initially derived when the silica percentage concept was originated from Reid and Cohen. Table 2-6 compares the accuracy of these methods of relating viscosity to composition.

Sage and McIlroy also made comparison of measured Tcv with the ASTM cone fusion temperature by adding 200^{o} F to ash softening temperature.

Ash composition and viscosity are equally important both in slag tap and pulverized coal fired boiler furnaces. Gronhovd and coworkers (1962) suggested that ideal slag should behave as a Newtonian fluid over a wide temperature range and should have a relatively low viscosity (less than 50 poisesss for a slagging fixed bed gasifier). Here viscosity establishes the rate of flow but Tcv determines whether the slag will continue to flow as it cools on leaving the hearth.

3) Ash fouling

Crossley and Marskell (1955) have classified the forms of fouling as follows:

a) Fused-slag deposits occurring principally on surfaces exposed to radiant heat transfer, such as on the furnace walls and the

Reproduced with permission of the copyright owner. Further reproduction prohibited without permission.

Table 2-6 Comparative reliability of method of predicting viscosity of coal ash slag from chemical composition

TEMP (°C)	Log Viscosity (poises), Calculated—Observed					
	Mean			Confidence Limits (0.05 level)		
	Reid and Cohen	Hoy et al.	Watt and Fereday	Reid and Cohen	Hoy et al.	Watt and Fereday
1200	−1.42	—	−0.024	± 0.52	—	± 0.29
1300	−0.031	0.182	−0.009	± 0.42	±0.31	± 0.24
1500	0.032	0.023	0.006	± 0.28	±0.25	± 0.23

(Watt and Fereday, 1969)

Reproduced with permission of the copyright owner. Further reproduction prohibited without permission.

first few rows of boiler or superheater tubes,

b) High temperature bonded deposits occurring on convection heating surfaces in regions of moderately high gas temperature, principally in the superheater, and

c) Low temperature deposits occurring on convection heating surfaces of economizer and air heater.

Any form of ash deposit that retards heat transfer or obstructs the flow of gases through the units of the firing system is considered to be fouling. It varies characteristically with firing method and with the nature of fuel. Physical erosion and chemical corrosion are operative in the period of ash fouling. The particle sizes vary from truly molecular gas and vapor through aerosol and microscopic suspensions to macroscopic and relatively coarse particles.

General description of ash fouling

a) Fused slag deposits

The formation of a slag deposit is caused by physical transportation of fused or partially fused particles entrained by the gas stream. When the particles strike the wall or tube surface, they are chilled and solidified. The strength of attach-

Reproduced with permission of the copyright owner. Further reproduction prohibited without permission.

ment is influenced by the temperature and physical contour of the surface, and by the direction, force of impact, and wetting characteristics of the slag. In slag-tap furnaces, firm attachment and complete coverage normally exist on the refractory surfaced stud-tube wall construction, frequently used in the combustion zone. Accumulation of wall deposit delays cooling with a resultant increase in the temperature of gases delivered to the superheater. This tends to raise final steam temperature and also causes deposits to advance into the cooler portions of the furnace.

b) High temperature bonded deposits

These deposits occur under some conditions on the superheater or reheater at a critical range of temperature appreciably below the fusion temperature of the ash. They may also cause corrosion of tubes operating at metal temperatures above 1150^{o} F. Several types of bonded deposits have been identified and are referred to as the alkali, calcium, phosphate, or silica types accroding to the principal bonding agent, although they may exist in combination. All appear to involve volatilization of elements from the ash and selective deposition upon or in the vicinity of the tube surface, thereby producing local concentration several

Reproduced with permission of the copyright owner. Further reproduction prohibited without permission.

times greater than their normal proportion in the ash.

c) Low temperature deposits

Deposits occurring in the cooler sections of the unit are caused primarily by the condensation of aqueous vapors and entrapment of fly ash. The dewpoint of acid or water in the gases determines the condensation on the surface of economizer and air heater. Condensation is aggravated by the presence of these deposits, since they impose a barrier to heat transfer but permit diffusion of vapors to the underlying cooled surface. The deposits may contain a great variety of elements and compounds but are commonly found to be high in water soluble sulfates of iron and aluminum.

4) Corrosion

Corrosion occurring on heat absorbing surface may be grouped as follows:

a) Low-temperature corrosion by sulfuric acid from the flue gases,

b) High-temperature corrosion of furnace walls, superheater, and reheater tubes by molten ash constituents. In either instance, corrosion necessitates periodic repairs or replacement of these

Reproduced with permission of the copyright owner. Further reproduction prohibited without permission.

parts, which is generally a time consuming and costly procedure. It is also important to note that corrosion limits the capacity and efficiency at which the boiler can be operated and in some instances causes unscheduled outages of equipment.

In both cases, sulfur content is the major source of the problem, either by formation of sulfuric acid vapor at low temperature or by forming trisulfate with alkali metals in high temperature environments. Even with coals containing as little as 0.3% sulfur, enough SO_3 can be present to form trisulfates. Coal preparation and chemical treatment of coal to lower the sulfur content will not eliminate metal wastage unless the sulfur is decreased to well below 0.3%. More effective would be the selective removal of sodium and potassium, which however is not considered economically feasible. Also, adjustment of the calcium and magnesium content of the coal ash by coal preparation can have a marked effect on superheater and reheater wastage. Fig. 2-6 shows the reactivity gain as a function of temperature for a mixture of Fe_2O_3 and Na_2SO_4. The reactivity with 30 ppm SO_3 present is much greater than that with 5.8% SO_2 alone. The problem of sulfuric acid formation, Fig. 2-7 summarizes a widely accepted relationship between SO_3 level and sulfuric acid dew point as influenced by water content in the flue gases. The

Reproduced with permission of the copyright owner. Further reproduction prohibited without permission.

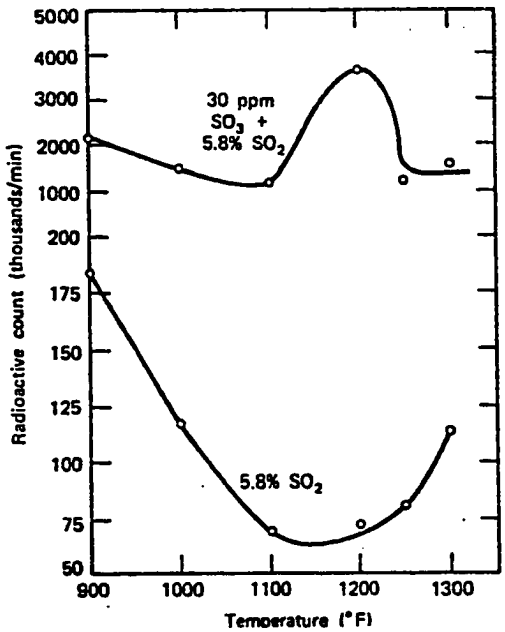

Figure 2-6 Reactivity of SO_3 and SO_2 with a mixture of Fe_2O_3 and Na_2SO_4 as a function of temperature. (Krause, et. al., 1968)

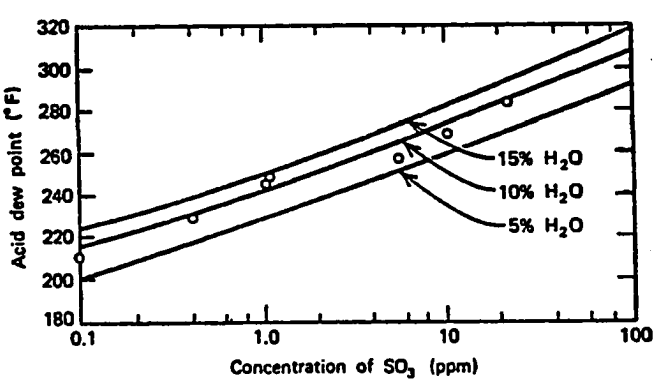

Figure 2-7 Dew point of SO_3 in flue gas.
(Reid, 1971)

Reproduced with permission of the copyright owner. Further reproduction prohibited without permission.

importance of these findings emphasizes the exceedingly low level of SO_3 required to approach the water dew point. Even with 0.1 ppm SO_3 the acid dew point is still 200° F when only 5% H_2O is present in the flue gases. Chemical reactions to capture SO_3 by adding limestone or dolomite or by the presence of slightly reducing flue gas conditions are necessary to achieve such low concentrations of SO_3 (Reid, 1971). Large boiler systems cannot generally reach these low levels; therefore an efficiency penalty is accepted by discharging the flue gas to the stack well above the acid dew point. The use of flue gas scrubbers may eliminate this acid dew point problem. It is worth noting, however, that attempts to meet environmental restrictions by the chemical cleaning of coal to reduce the sulfur content to a point below the levels of conventional coal-cleaning systems may still put enough SO_3 into the flue gas to raise the acid dew point significantly.

C) Effect of coal ash on conversion systems

I) ash related problems during gasification

II) mineral matter and liquefaction of coal

III) effect of mineral matter on catalysts

IV) mineral matter as a catalyst in noncatalystic system

Reproduced with permission of the copyright owner. Further reproduction prohibited without permission.

I) Ash related problems during gasification

The problems of old fixed-bed gasifiers are comparable to clinkering troubles in stokers. Both limit fuel bed temperature; the use of high ash fusion coals can solve these problems. For slagging gasifiers, Hoy and coworkers (1965) found potential fluxing of iron oxides in slag and consequent conversion to metallic iron, under reducing conditions in a gasifier. This effect leads to a loss of flux and an increase in slag viscosity, or would mean that the gasifier needs to have CaO added as flux in order to tap the slag satisfactorily.

Alkalis also cause trouble by attacking the refractory linings used in gasifiers. The problems are so severe that even SiC can not withstand the flowing slag in the vicinity of the taphole.

II) Mineral matter and liquefaction of coal

Gorin (1962) classifies mineral matter in coal into two catagories. The first category includes clay minerals, pyrite, quartz, gypsum, and calcite which occur as discrete particles in the matrix of organic matter. The second category includes inorganic salts of organic acids present in the coal, and organic chelates of refractory oxides such as TiO_2, $Al_2O_3$and SiO_2

Reproduced with permission of the copyright owner. Further reproduction prohibited without permission.

as well as chelates of trace elements. The inorganic salts usually comprise the major portion of alkaline earth metals present in the coal. Table 2-7 shows the composition of ash of coals with various rank and the percentage removal of various oxides with sulfurous acid after 60 min. residence time at ambient temperature.

It is apparent that alkai and alkaline earth metals are easily removed and become important components of the mineral matter as coal rank decreases. The major portion of potassium is apprently tied up with clay minerals such as illite in a form that is not readily extractable. The iron removed from subbituminous coal is apparently present as organic salt or readily extractable inorganic form.

Mineral matter in the extract derived by liquefaction may be characterized both by chemical analyses and by ash size distribution. Data provided in table 2-8 shows that the composition of the coarse ash in the extract is substantially equivalent in chemical composition to the original coal ash. The fine ash, however, is of quite different composition. Titania enrichment is likely due to the presence of organo-titanium chelated compounds of unknown structure. The CaO and alkali metals are

Reproduced with permission of the copyright owner. Further reproduction prohibited without permission.

Table 2-7 Ash composition of coals and extraction with sulfurous acid

Coal:	Hillsboro	Browning Mine	Colstrip	South Gillette	Glenharold
Mesh size:	−100	−100	−14	−14	−14
Type	Illinois bituminous	Utah bituminous	Montana subbituminous	Wyoming subbituminous	North Dakota Lignite
			Extraction (% removed)		
Total ash	19	37	36	39	62
Na_2O	82	8	69	96	98
K_2O	4	7	33	34	68
CaO	98	92	84	82	85
MgO	11	78	91	85	88
Fe_2O_3	9	23	11	63	92
			Ash Composition of Feed Coal (wt % of Ash, oxidized and SO_3-free basis)		
Na_2O	1.6	3.3	0.2	1.5	10.5
K_2O	1.7	0.2	0.1	0.6	0.9
CaO	7.1	18.6	15.4	22.0	36.4
MgO	0.9	5.0	6.0	3.6	7.1
Fe_2O_3	23.8	5.6	4.1	4.1	8.2

(Gorin, 1975)

Reproduced with permission of the copyright owner. Further reproduction prohibited without permission.

Table 2-8 Chemical composition(wt%) of coal and extract ash

	Ireland Mine Coal	Filtered Extract	
Size:	All > 1 μm	+ 1.2 μm ash	< 0.01 μm ash
Total ash (wt %):	13.6	0.034	0.103
Chemical Composition:			
$Na_2O + K_2O$	2.3	2.8	6.0
CaO	5.4	5.8	22.9
MgO	1.2	4.4	3.5
Fe_2O_3	23.7	14.2	5.3
Al_2O_3	16.9	15.6	17.5
SiO_2	49.3	53.4	14.6
TiO_2	1.2	1.8	30.2

(Gorin, 1969).

Reproduced with permission of the copyright owner. Further reproduction prohibited without permission.

likely present as soluble complex organic acids.

III) Effect of mineral matter on catalysts

The deactivation of catalysts in the H-coal and Synthoil processes or in the CSF process is discussed by Kang, Johanson (1976) and Kovach, Bennett (1975). They conclude that the deactivation mechanism of catalysts is caused by the deposition of metals in the pores of the catalyst. The metals occur principally as organometallics or soluble ash component such as alkali and alkaline earth salts. Titanium is an excellent indicator in identifying the deposition profile of metals on catalysts, both due to the ease of its detection and also because it is one of the principal elements present in the coal as an organic chelate. It is also worth noting that the rate of decline of catalyst activity is not only a function of the total soluble ash, but also varies with the proportion of alkali and alkaline earth oxides in the soluble ash.

IV) Mineral matter as a catalyst in noncatalitic system

In general, the catalytic studies of mineral matter in liquefaction of coal show that weight percent mineral matter is strongly correlated with conversion as shown in. Fig. 2-8

Reproduced with permission of the copyright owner. Further reproduction prohibited without permission.

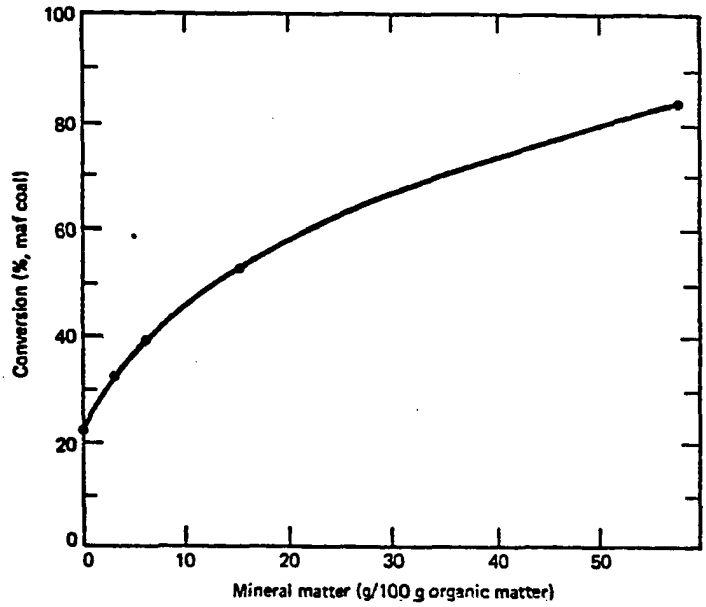

Figure 2-8 Relation between mineral matter content and conversion hydrogenation of North Assam coal. (Mukherjee and Choudhury, 1976)

Reproduced with permission of the copyright owner. Further reproduction prohibited without permission.

(Mukherjee,1976). Iron sulfide is the major catalytic component, while titanium and kaolinite also are demonstrated to be mildly catalytic. The study also noted that the float-sink fractions, enriched in mineral matter, were also enriched in the refractory petrographic component, inertinite. Inspite of this, better conversion was obtained with coal containing high ash than with the low-ash materials enriched with the more reactive component, vitrinite. Hydrocarbon Research Inc. and CCDC (Gorin,1977) also give bench scale data on hydroextraction which indicates no simple relationship between the iron content and rank of the feed coal and the hydrogen consumption. Intensive studies were conducted by Gulf Research and Pennsylvania State University (Given, 1975) on the effect of coal rank and petrographic composition on conversion using a catalyst. An autoclave procedure was separately conducted with and without anthracene oil as a vehicle.

High-volatile A,B and C bituminous coals generally gave the best conversion by both procedures, but no relationship between liquefaction response and coal rank or geological age was evident. Bituminous coal from the State of Washington gave a favorable response to liquefaction, and the exceptionlly high mineral matter content may explain this. A North Dakota lignite

Reproduced with permission of the copyright owner. Further reproduction prohibited without permission.

for a sodium-enriched and sodium-free feed pretreated gave 96% and 97% conversions respectively by the Gulf procedure. The sodium enriched lignite gave oil of low viscosity and benzene-insoluble content than the sodium-free lignite. Figures 2-9 and 2-10 by Given show that the subbituminous and HvAb coal gave fair correlation between liquefaction behavior and concentration of reactive macerals. In the case of lignite, no correlation of liquefaction behavior with macerals was found. The results were obtained with a high-ash, fusinite-rich, 1.4 specific gravity sink sample. Again, iron rich minerals and high ash content had a catalytic effect in liquefaction.

D) The trace elements of coal

The importance of trace elements in coal or coal ash is due to the fact that the trace elements in coal ash are enriched 10 to 185 times compared to the concentration in the earth's crust. These are Li, Sr, Ag, As, Bi, B, Ga, Ge, La, Hg, Pb, Sb, Sn, Zn and Zr.(Goldschmidt,1950 and Headlee and Hunter, 1951). Table 2-9 modified from Krejci-Graf (1972). gives the magnitude of enrichment of trace elements in coal ash.

Trace element recovery and environmental impact

Reproduced with permission of the copyright owner. Further reproduction prohibited without permission.

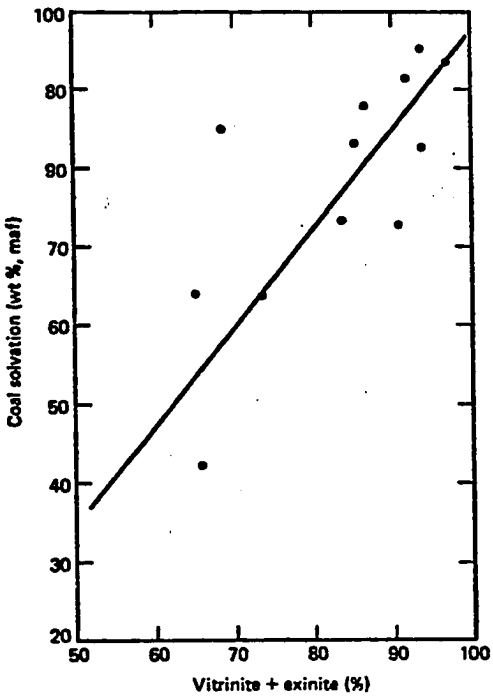

Figure 2-9 Coal solvation versus reactive maceral:New Mexico subbituminous coal from the Blue seam Mckinley Mine.
(Given, 1975)

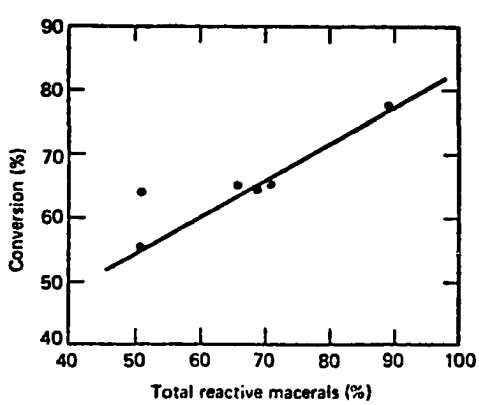

Figure 2-10 Solvation of lithotypes from the Elkhom No.3 seam, HvAb Kentucky coal.
(Given, 1975)

Reproduced with permission of the copyright owner. Further reproduction prohibited without permission.

Table 2-9 Enrichment of elements in coal ash (ppm)

Element	Earth's crust (average)	Pelitic sediments	Max. contents in coal ash
Li	65	46	960
Be	6	<4	2800
B	10	310	8600
Sc	5	6.5	400
Ti	4400	4300	20000
V	150	120	11000*
Cr	200	550	1200
Mn	1000	620	22000*
Co	40	8	2000
Ni	100	24	16000
Cu	70	192	4000*
Zn	40	200–1000	10000*
Ga	19	50	6000
Ge	7	7	90000
As	5	~5	8000
Rb	280	300	33
Y	28	28	800
Zr	220	120	5000
Nb	20	–	2
Mo	2.3	–	2000*
Ag	0.02	0.05	5–10
Cd	0.18	0.3	80
In	0.1	0.5	2
Sn	40	40	6000
Sb	1	3	3000
I	3	0.3	950
Cs	3.2	12	4
La	18	18	31
Ta	2.1	–	0.1
Pt	0.005	–	0.7
Au	0.001	–	0.2–0.5
Hg	0.5	0.3	50
Tl	1.3	2	25
Pb	16	20	1000*
Bi	0.2	1	200
U	4	1.2	600*

* Higher values are probably due to secondary enrichment.

(Krejci-Graf, 1972)

Reproduced with permission of the copyright owner. Further reproduction prohibited without permission.

The enrichment of trace elements in coal ash prompted attempts to recover certain useful elements. One early effort was in the recovery of Ge, based mostly on the finding that germanium present in coal was concentrated in the fly ash. The enrichment factor ranged from 3.3 to 18.7(Corey et al.,1959). The highest concentration was found in fly ash from a chain-gate-fired boiler furnace with 530 ppm Ge, and from a cyclone furnace with 290 ppm ge. The germanium content of coal is variable and selective mining for this purpose is not economically feasible. No commercial germanium industry using coal ash residues has developed.

Zinc in the form of sphalerite has been found in Illinois coals at concentrations greater than 5000 ppm(J.R.Hatch, et al., 1976). Separation of sphalerite from the coal by washing is practical and has been suggested as an economically attractive process. Recovery of Selenium in fly ash has also been suggested, since there are limited Selenium sources to meet the commercial demand.

In general, coal ash may not offer much promise as a source of useful products except those mentioned above. There seems to be little possiblility that the inorganic matter in coal will find a market as a source of useful raw materials in the near fu-

Reproduced with permission of the copyright owner. Further reproduction prohibited without permission.

ture.

On the other hand, the major potential environmental impacts of residues and ash associated with coal preparation results from the leachability of trace contaminants and their infiltration into groundwater and surface water. There is also some concern on the possibility of resuspension of collected fly ash in the atmosphere during disposal. This is because not only does some fly ash contain potentially respirable small particles, but also because some trace elements are more highly concentrated in these particles (Natusch, et al.,1977).

If all the trace elements in coal ashes were assumed to be mobilized into water, most ashes would be classified as hazardous, requiring expensive disposal techniques. Fortunately, not all materials are soluble in water and even those that are mobilized leach at different rates and to different extents. Most of the trace elements in leachates are fixed and retained in soils, (NRC,1977) a condition that would minimize their migration to groundwater. However, some of the trace ions can be taken up by plants or moved with water that is evaporated from the upper layers of the soil. Some trace elements found in coal are toxic, even at fairly low concentration , to both terrrestrial and

Reproduced with permission of the copyright owner. Further reproduction prohibited without permission.

aquatic amimals and to plant species. Other trace elements are essential to plant growth, but they are toxic in amounts only slightly higher than those in the environment, and could persist for extended periods. The effect on animals and plants is cummulative and will often manifest itself only after years of exposure. Control of emissions is possible through existing technology, modifications in the design of processes, and changes in operating procedures (ERDA, 1977). More data are needed to evaluate carefully the control options and to improve them, if necessary.

Reproduced with permission of the copyright owner. Further reproduction prohibited without permission.

CHAPTER 3

SAMPLE COLLECTION

Coal is widely distributed in Alaska and may be divided into five major coal districts:

A) North Slope: Artic slope north of the Brooks mountain range.

B) Interior: between the Brooks Range and Alaska Range.

C) Cook Inlet: from Alaska Range South to Gulf of Alaska.

D) The Alaska Peninsula region: Alaska Peninsula and Aleutian Islands.

E) Southeastern Alaska: Bearing river coal field and related fields.

The samples used for this research program were collected from districts A through D. The samples range in rank from high volatile bituminous to subbituminous C. These coals occur in rock formations of Tertiary or Cretaceous age. All of Alaska's coals are limited to those two systems. Seams chosen for this study were the most accessible, each has the best commercial potential within each of the coal districts.

The following is a description of each of the localities and seams sampled:

A) North Slope--- Northern Alaska Coal field, Cape Beaufort No. 7

Reproduced with permission of the copyright owner. Further reproduction prohibited without permission.

bed.

The Cape Beaufort area has been drilled by the U.S. Geologicl Survey and the U.S. Bureau of Hines in greater detail than any other area in the field. Coal occurs in the nonmarine Corwin formation of Creataceous age. No. 7 bed is the thickest seam in the area. The sample UA 139 was collected from a trench cut by U.S. Bureau of Mines with a bulldozer. The sample has a lower heat value (Btus/lb) than those samples collected by drilling on a moisture and ash free basis (Warfield,1969). The rank of coal is high volatile C bituminous (Rao,1982a).

B) Interior Alaska--- Nenana coal field, Usibelli Coal Mine No.3 seam.

The Nenana coal field is located about 110 miles south of Fairbanks on the Parks Highway at Healy. The No. 3 seam is currently being mined by the Usibelli Coal Mine. The coal seam is in the Suntrana formation of the Coal Bearing group exposed on lower Lignite Creek. The formation consists of sandstones, siltstone, claystone, shale and numerous thick coal beds. Total proven reserves in the Lower Lignite Creek area are 80 million tons with a resource potential of 250 million tons. (Denton, 1980)

Reproduced with permission of the copyright owner. Further reproduction prohibited without permission.

The sample UA 130 was collected from lower lignite Creek No. 3 seam, Poker Flat Pit, Usibelli Coal Mine. The rank of coal is subbituminous C.

--- Matanuska coal field, Chickaloon formation, Evan Jones mine, No. 5 bed.

The Matanuska coal field is located about 45 miles northeast of Anchorage on The Glenn Highway. Coal was mined extensivley in this area until the energy supply in the Anchroage area was replaced by natural gas. The coal seams are limited to the Chickaloon formation of Tertiary age. This formation consists of nonmarine rocks that include all gradations from coarse sandstone and conglomerate to claystone (Barnes, 1956). Washability studies for the Evan Jones coal mine in the field were conducted by Geer and Yancy of U.S. Bureau of Mines in 1962. Additional washability studies of 5 coal seams from the aboundand Evan Jones mine pit were completed by Rao (1982). The rank of coal increases from high volatile B bituminous in the Wishbone Hill district to high volatile A bituminous at the Castle Mountain mine to anthracite at Anthracite Ridge. The sample UA 147 was collected from No.5 bed of Evan Jones mine in the Wishbone Hill district.

Reproduced with permission of the copyright owner. Further reproduction prohibited without permission.

C) Cook Inlet--- Yentna coal field, Johnson Creek. , and Beluga coal field, Green seam.

The Yentna coal field is one of three coal fields in the Cook Inlet sedimentary basin. The coal seams in the field are confined to Tyonek formation in the Kenai group which lies unconformably over a series of metamorphic and igneous rocks of early Jurassic to Cretaceous age. There are three seams outcropping along Johnson Creek. However, five to seven seams ranging from 10 to 40 feet in thickness have been revealed by drillhole data. (Blumer, 1980) The sampled seam is the thickest of the three beds outcropping.

The Beluga coal field is the most important of three coal fields in the Cook Inlet sedimentary Basin . The field may be subdivided into three coal bearing regions. Green seam is one of five major seams (Barnes, 1966) in the Chuitna River basin which lies about 50 miles west Anchroage. The sample UA 152 was collected from a pit dug on Green seam by Placer Amex, inc., on their lease holding for shipment of a 2000 ton bulk sample to Japan for testing. Beluga Coal Company estimates the minable reserves in their leased area of Chuitna Basin total approximately 200 million tons of near surface coal on the west side of

Reproduced with permission of the copyright owner. Further reproduction prohibited without permission.

the river. Reserves in the Diamond Alaska Coal Co. lease holding are estimated at 350 million tons at a cumulative strip ratio of 4.4.

D) Alaska Peninsula region: Chignik coal field, Chignik river Mine.

The Chignik coal field is on the west shore of Chignik Bay. The coal bearing Chignik formation of late Cretaceous age is confined largely to a northeastward tending belt about 25 miles long, and 1 to 3 miles wide along the northwest shore of Chignik Bay (Barnes, 1967). Coal mines in Herendeen Bay, Chignik and Unga Island were operated from around 1880 to 1914 to support the Chignik fish cannery. The sample UA 136 was collected from the mine tunnel of the Chignik River Mine that operated from 1893 to 1911.

Reproduced with permission of the copyright owner. Further reproduction prohibited without permission.

CHAPTER 4

SAMPLE PREPARATION AND ANALYSES

Raw coal samples were crushed to 1-1/2 inches and 14 mesh sizes. Minus 100 mesh material was removed from the 1-1/2 inches crushed sample, leaving the coarse fraction for float-sink testing in 60 liter containers. 14 mesh x 0 samples were separated in glass separatory flasks with ground taper joints. Float-sink separations were made at 1.3, 1.4 and 1.6 specific gravities, using perchlorethylene-naptha mixtures as heavy liquid. The air dried products were first crushed in a hammer mill to 14 mesh and pulverized to 60 mesh for analysis. Figure 4-1 shows the flowsheet used in the laboratory for processing the samples. Washability analyses for the samples used were reported by Rao and Wolff (1982a, 1982b). Laboratory procedures used in this investigation are as follows:

Ashing Technique

Medium Temperature Ash (MTA)

Twenty grams of minus 60 mesh pulverized sample were weighed into quartz combustion boats and oxidized 1020^{o} F while maintaining a positive flow of air. A 24-hour ashing time was allowed for all samples. After completion of ashing, the

Reproduced with permission of the copyright owner. Further reproduction prohibited without permission.

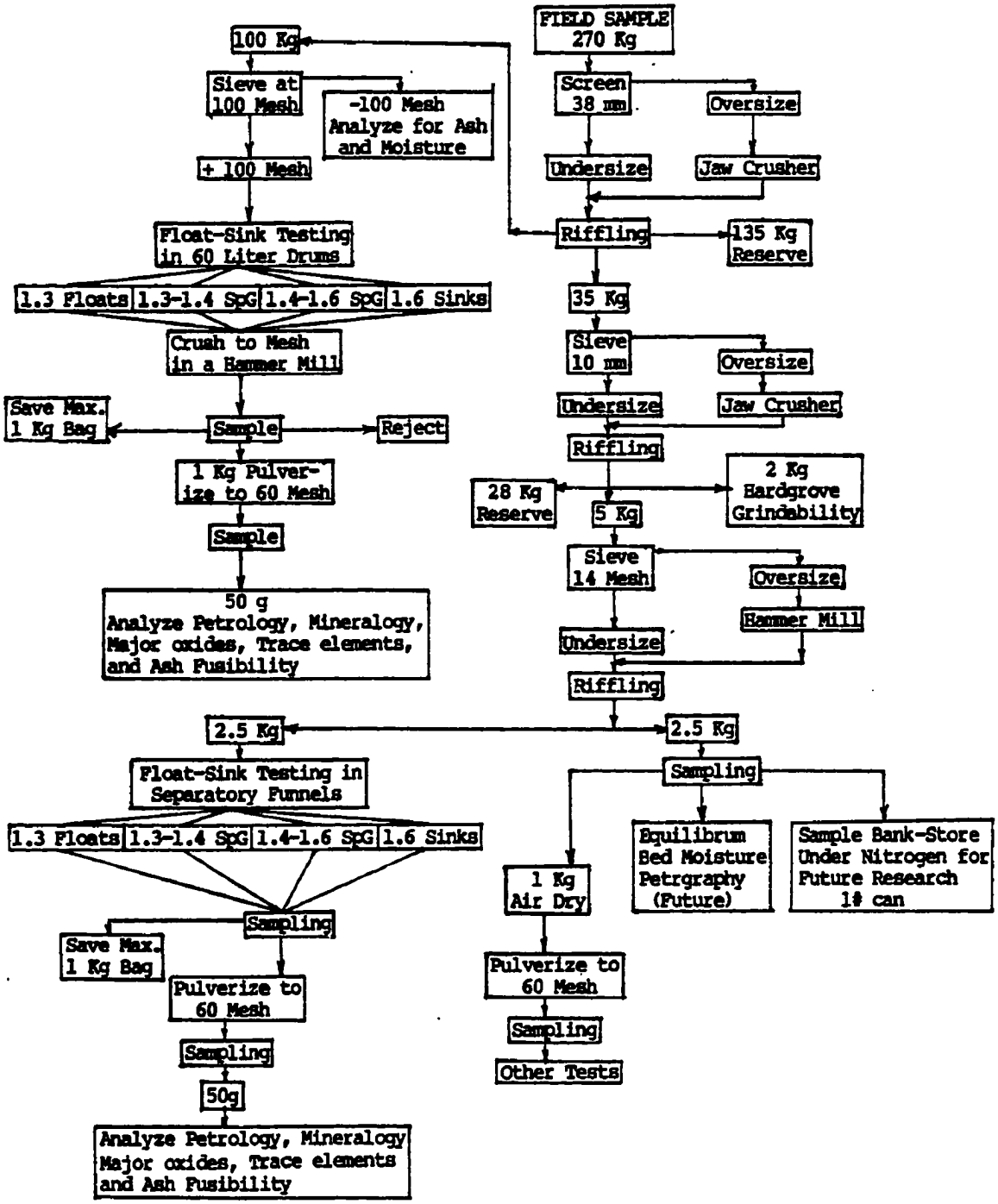

Figure 4-1 Flowsheet for washability of processing samples

Reproduced with permission of the copyright owner. Further reproduction prohibited without permission.

combustion boat was weighed and the ash was stored in air-tight bottles for trace element analyses, using inductively coupled plasma spectrochemical analyses. The medium temperature ash percentage is higher than that of high temperature ash since it has more undecomposed mineral matter, particularly carbonates, and the sulfur was retained as sulfate.

Low temperature ash (LTA)

One gram of 60 mesh sample was ashed in a low temperature asher (LFE Corporation) using plasma exicited oxygen at a temperature of less than 212 ^{o} F. The sample was stirred several times during ashing period, until the ash weight loss is less than 10mg in an 8 hour ashing period. The average ashing time for subbitumious C coals was five days, whereas high volatile B bitumious coals needed only two and one half days. These samples were used for XRD (X-ray diffraction) and infrared analyses for the determination of mineral species.

Reproduced with permission of the copyright owner. Further reproduction prohibited without permission.

A) Medium temperature ash---Chemical constituents of ash

I) XRF pellet preparation

Medium temperature ash of the coal samples is pulverized to minus 150 mesh and dried for 60 minutes at 175° F. A Pt/Au crucible is weighed and the weight is recorded as "CRWT". 6.0000gms of lithium tetraborate is weighed into the Pt/Au crucible and the combined crucible + lithium tetraborate weight is recorded as "LIBWT". The dry sample is rolled to homogenize and exactly 1.0000gms of sample is immediately weighed into the crucible containing lithium tetraborate. This weight is recorded as "SPLWT". 1.5000 grams lithium nitrate is weighed into the crucible and the combined weights of flux + sample + lithium nitrate are recorded as "OXWT". The crucible charge is carefully and thoroughly mixed with a small spatula. Care is taken not to scratch the soft Pt/Au crucible. With a small spatula, 4 small pits are formed in the crucible charge. One drop of HBr is added to each pit and covered over with the surrounding sample charge. A clean cover is placed on the crucible and the covered crucible is set in the puff furnace. After the crucible is removed from the puff furnace the crucible lid is carefully removed. The crucible and bead are immediately weighed without

Reproduced with permission of the copyright owner. Further reproduction prohibited without permission.

removing the bead from the crucible. This weight is recorded as "BDWT". The bead is labled on its concave side and a TEK culture dish lid. A cellophane-tape cradle is made in the TEK dish and the bead is placed in it. A white polyester 3M scouring pad and ALCONOX is used to wash the Pt/Au crucibles and lids between runs. Residue that will not wash out with this system must be dissolved out by hot HCl. A slight residue on the cover may build up through the day in spite of washing. This residue should be dissolved off by placing the affected covers in HCl and stirred overnight.

II) XRF spectrometry analyses

A wavelength dispersive x-ray spectrometer is used for the determination of major oxides. The radiation emitted by the sample is diffracted by lattice planes of known d spacing in a single crystal. Radiation of a single wavelength is reflected for each angular setting of the crystal, and the intensity of this radiation is measured with a suitable counter (both scintillation and sealed gas proportional counter). A wavelength dispersive spectrometer is also called a crystal spectrometer. The sample is bombarded with x-rays. The primary radiation causes the sample to emit secondary fluorescent radiation, which

Reproduced with permission of the copyright owner. Further reproduction prohibited without permission.

is then analyzed in a spectrometer. In automatic single channel spectrometers, the angular position 20 at which wavelength will be reflected, are preset. The characteristic wavelength is automatically calculated by computer depending on the Bragg angle and the interplanar spacing of the crystal.

III) Digestion with Hydrofluoric Acid

A sample of 0.5 grams of coal ash is weighed and transferred to a 3" diameter Teflon evaporating dish. The sample is moistened with 2 ml distilled water. After an addition of 4 ml perchloric acid, the dish is heated on a hot plate until nearly dry. The dish is cooled and 1 ml perchloric acid and 10 ml HF are added and evaporated to near dryness. The dish is cooled and 1 ml $HClO_4$ and 5 ml 5% boric acid solution are added and swirled to make sure that all the sample is loosened from the bottom of the dish. Any sticking residue is loosened with a polyethylene covered rod. The dish is now heated until dense fumes evolve, without allowing the residue to dry. The dish is cooled and the residue is taken into solution with 20 ml 25% HCl and made up to 50 ml.

IV) Inductively Coupled Argon Plasma Spectrometer

Reproduced with permission of the copyright owner. Further reproduction prohibited without permission.

A new source used for atomic emission is the inductively coupled argon plasma (ICP), which has eliminated many of the problems associated with past emission sources and caused a dramatic increase in the use of emission spectrometry. The ICP is an argon plasma maintained by the interaction of an RF field and an ionized argon gas and is reported to reach temperatures as high as 10,000 degree K, with useful temperaturess between 5,500 and 8,000 degree K. These temperatures allow complete atomization of elements, thus minimizing chemical interference effects.

The technical advantages of ICP compared to atomic absorption

a) Refractory elements can be determined. Uranium, zirconium, phosphorus, boron, and other rare earth elements can be determined routinely by ICP.

b) ICP has fewer chemical interferences. This is directly attributable to the extremely high plasma temperature and chemically inert atmosphere. The higher temperature causes more complete dissociation of the sample and results in less chemical interference.

c) No ionization interferences. In classical flame atomization, the higher the temperature, the greater the degree of ionization associated with a determination. However, the electron-rich na-

Reproduced with permission of the copyright owner. Further reproduction prohibited without permission.

ture of the plasma reduces ionization interferences and the addition of ionization suppressants is not required as with flame atomic absorption.

d) Wide linear working range. The sample is confined to a narrow stream within the plasma, resulting in an optically thin emission source. Therefore, the linear working range is extended several orders of magnitude beyond the range achieved with atomic absorption.

e) Improved detection limits. For most elements, detection limits are better for ICP emission than for flame AA.

Compared to AA, ICP also has its drawbacks:

a) Higher detection limits. Generally, furnace AA detection limits are 10 to 100 times better than ICP.

b) Less precision. With ICP, using typical operating conditions, a coefficient of variation in the range of 2.0 to 3.0% is obtainable even though significant improvements have been made in the sample introduction procedure, while a coefficient of variation of less than 0.3% is attainable with flame atomic absorption.

c) Spectral interference. Atomic absorption is virtually free of spectral interferences because of the specificity of the light sources. The primary light source only emits a limited number of

Reproduced with permission of the copyright owner. Further reproduction prohibited without permission.

lines which are not very close to each other, in contrast with ICP where line broadenings, direct line coincidences, and near spectral overlaps exist. However, with careful instrumental design, an optimal wavelength selection system, and accuate background correction, those interferences can be minimized in ICP.

Reproduced with permission of the copyright owner. Further reproduction prohibited without permission.

B) Low temperature ash---Mineralogy of coals

I) XRD analyses of low temperature ash

An internal standard method recommended by Rao and Gluskoter (1973) was used for the quantitative analysis of minerals in low temperature ash. An X-ray diffraction system with CuKa Ni-filtered radiation at 30 Kv and 30 ma was used.

Mineral matter residue obtained from low-temperature ashing was first ground in an agate mortar to minus 200 mesh. Finely powered pure fluorite equivalent to 10% by weight of total sample mixture was added to sample as an internal standard. The mixture was placed in a mortar with alcohol and ground to almost minus 400 mesh or finer.

The back-packed cavity mount technique described by Rao and Gluskoter (1973) was used in order to avoid orientation of powdered grains along the preferred cleavage faces of minerals.

A preliminary scan of the 52 samples from 2 to 40 degrees (2θ) revealed that the minerals in the samples are quartz, calcite, dolomite, siderite, plagioclase, kaolinite, illite, pyrite and bassanite. Two series of standard mixes were prepared. The first set (standard QCD) of standards consisted of quartz, cal-

Reproduced with permission of the copyright owner. Further reproduction prohibited without permission.

cite and dolomite, the second set (standard PSP), of plagioclase, siderite and pyrite.

An internal standard of 0.1 grams of fluorite powder, and a diluent of 0.4 grams of clay mixture containing equal amounts of kaolinite, montmorillonite and illite were added to the standard mixture to total 1 gram (table 4-1). The mixtures were ground with alcohol to minus 400 mesh. The mounted standards were x-rayed from 20 to 40 degrees of 2θ with a scanning speed of 1/2 degree per minute and a chart speed of 1/4 inch per minute for accuate peak-height. Peak-height intensities of each mineral were measured in recorded chart units with 1000 counts full scale. Two slides were prepared for each sample and each slide was x-rayed twice. An average value of the peak-height of the four reading was used. The reflections of minerals used for peak-height measurements were quartz (101,26.6), calcite (104,29.4), dolomite (104, 31), siderite (104,32), plagioclase (002,27.5), and flourite (111,28.2).

The calibration curves for these minerals are constructed by plotting the respective peak-height intensity ratio with flourite as the ordinates and percentage of the respective minerals in the standard as the abscissa (Figures 4-2 to 4-6).

Reproduced with permission of the copyright owner. Further reproduction prohibited without permission.

Reproduced with permission of the copyright owner. Further reproduction prohibited without permission.

Table-4-1I
Preparation of standard and calibration curves for plagioclase and siderite for analysis by X-ray diffraction

	Weight percent of mineral in standard mixtu					Peak height ratio	
Mixture Number	plagio-clase	side-rite	pyrite	Fluo-rite	Clay* Mixture	R_{pf}	R_{sf}
PS1	0	40	10	10	40	0.00	5.43
PS2	5	30	15	10	40	0.40	4.07
PS3	10	20	20	10	40	0.70	1.67
PS4	15	10	25	10	40	1.00	1.10
PS5	20	0	30	10	40	1.50	0.00

* diluent- A mixture of montmorillonite, kaolinite and illite in equal parts.

Reproduced with permission of the copyright owner. Further reproduction prohibited without permission.

Table-4-III

Preparation of standard and calibration curves for quartz, calcite and dolomite for analysis by X-ray diffraction

Mixture Number	Weight percent of mineral in standard mixture					Peak height ratio		
	Quartz	Calcite	Dolomite	Fluorite	Clay* Mixture	R_{qf}	R_{cf}	R_{df}
QCD1	40	0	10	10	40	3.43	0.00	0.76
QCD2	30	0	20	10	40	2.76	0.00	1.60
QCD3	20	30	0	10	40	1.59	2.38	0.00
QCD4	10	0	40	10	40	1.11	0.00	3.11
QCE5	10	20	20	10	40	1.11	1.45	1.60
QCD6	0	40	10	10	40	0.00	3.09	0.76
QCD7	10	10	30	10	40	1.11	0.74	2.14

* diluent- A mixture of montmorillonite, kaolinite and illite in equal parts.

Reproduced with permission of the copyright owner. Further reproduction prohibited without permission.

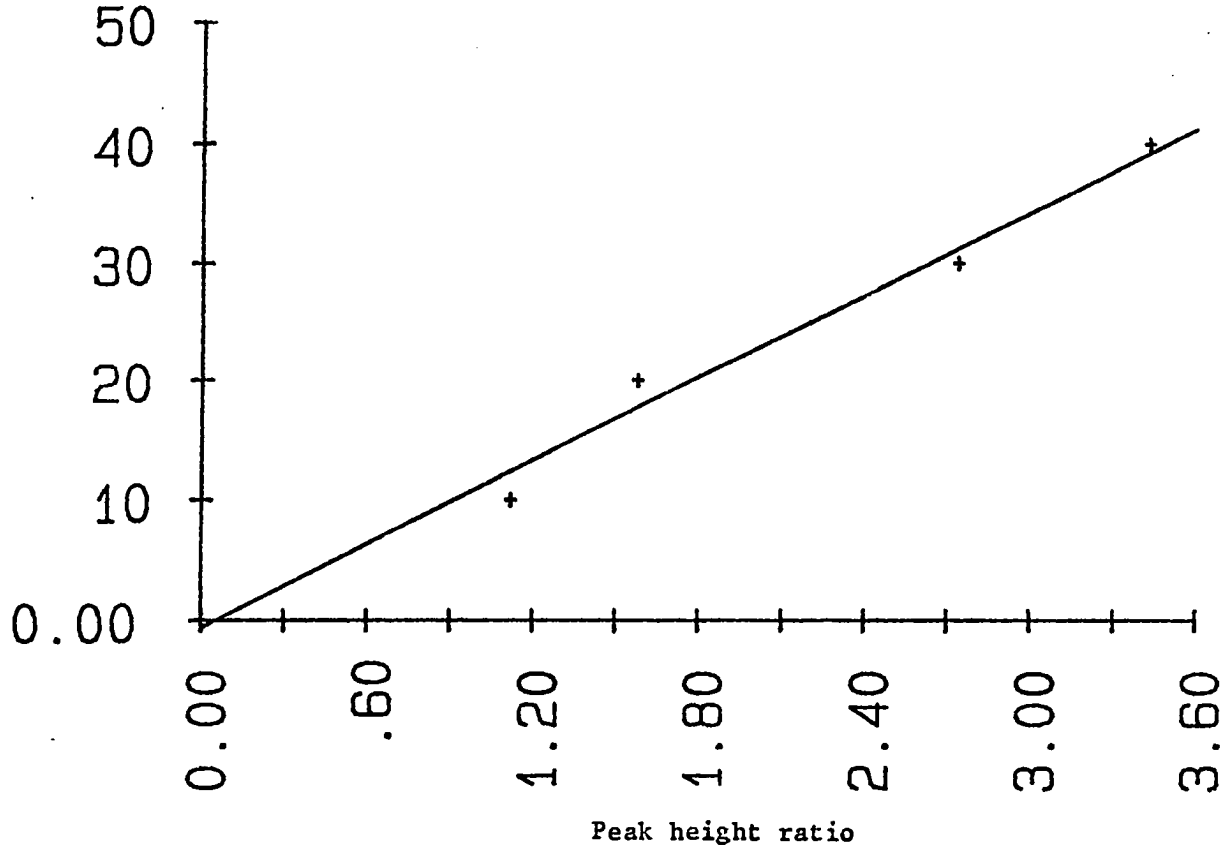

Figure 4-2 Calibration curve for the determination of guartz by X-ray diffration

Reproduced with permission of the copyright owner. Further reproduction prohibited without permission.

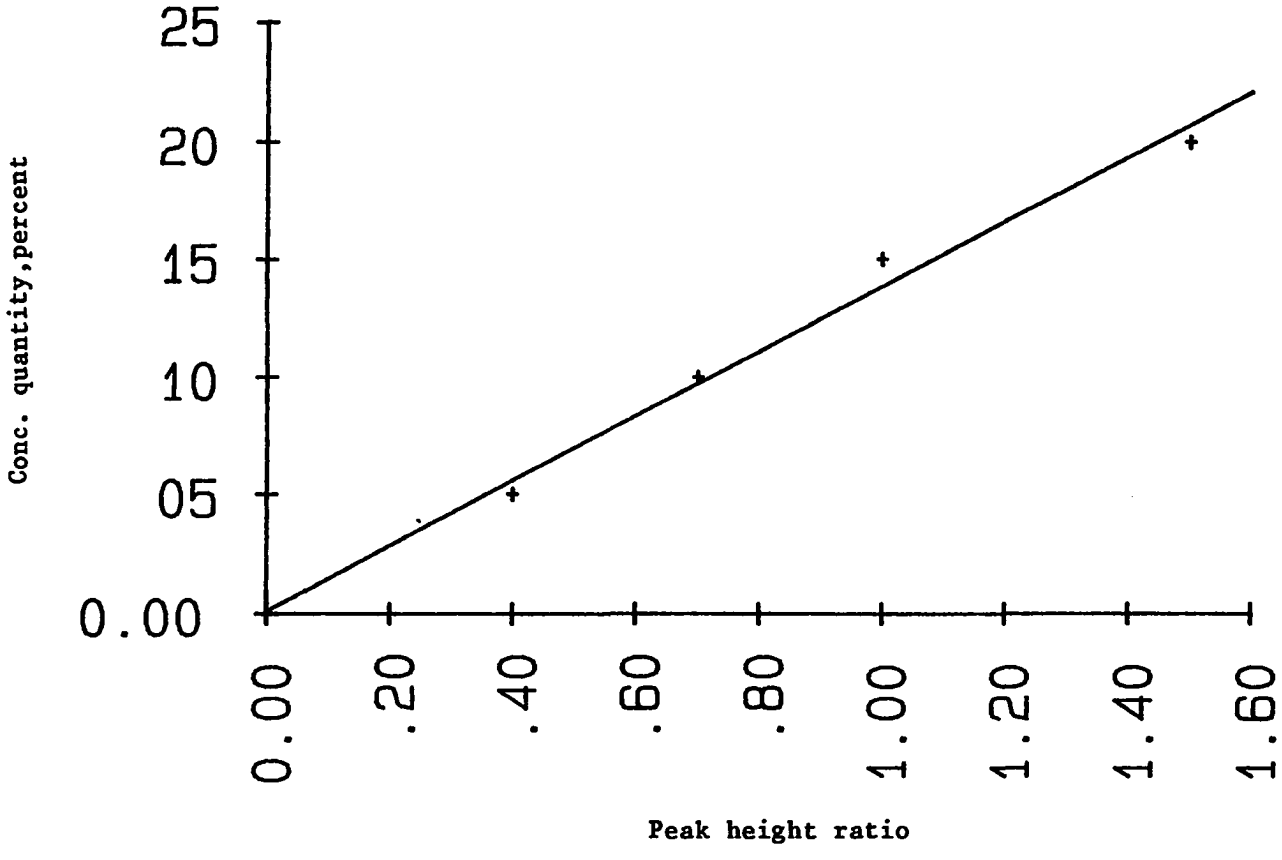

Figure 4-3 Calibration curve for the determination of Plagioclase by X-ray diffraction

Reproduced with permission of the copyright owner. Further reproduction prohibited without permission.

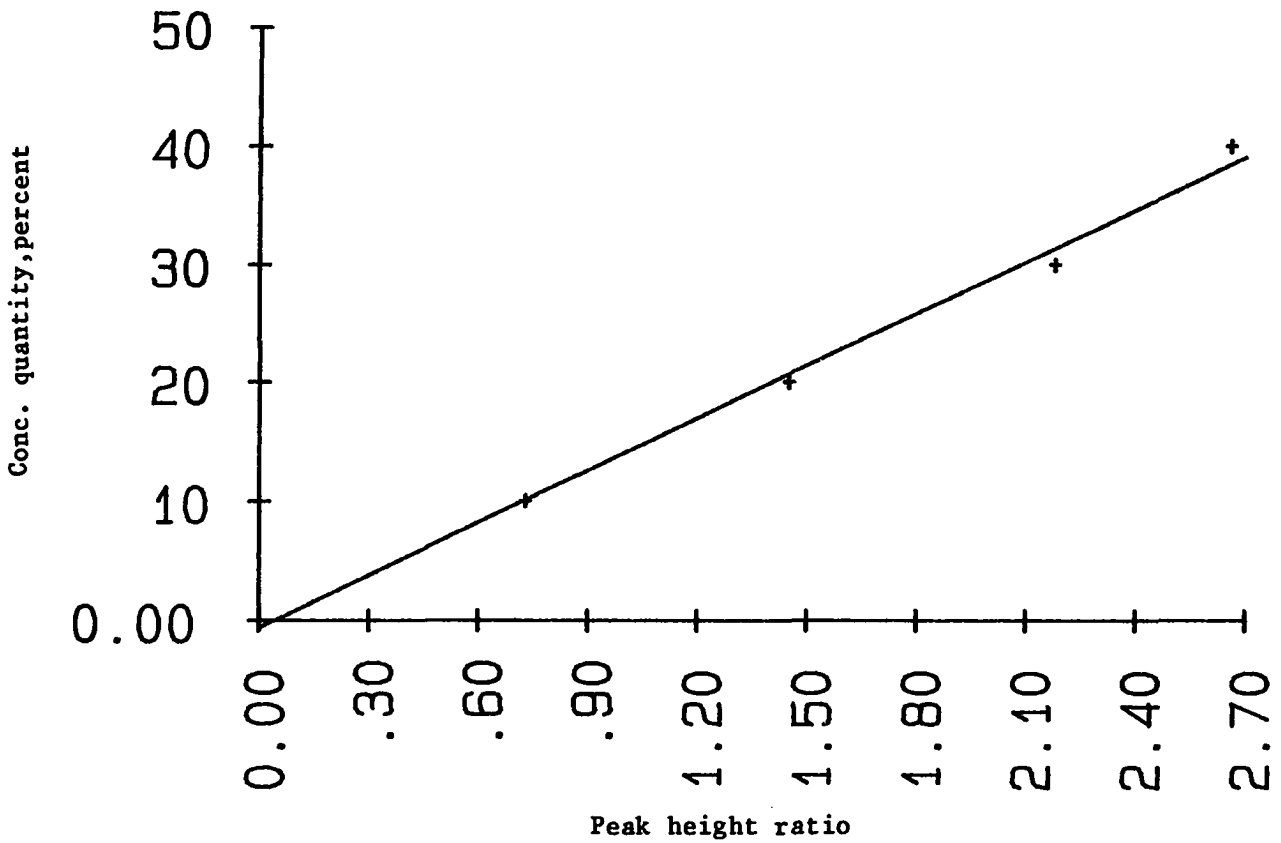

Figure 4-4 Calibration curve for the determination of calcite by X-ray diffraction

Reproduced with permission of the copyright owner. Further reproduction prohibited without permission.

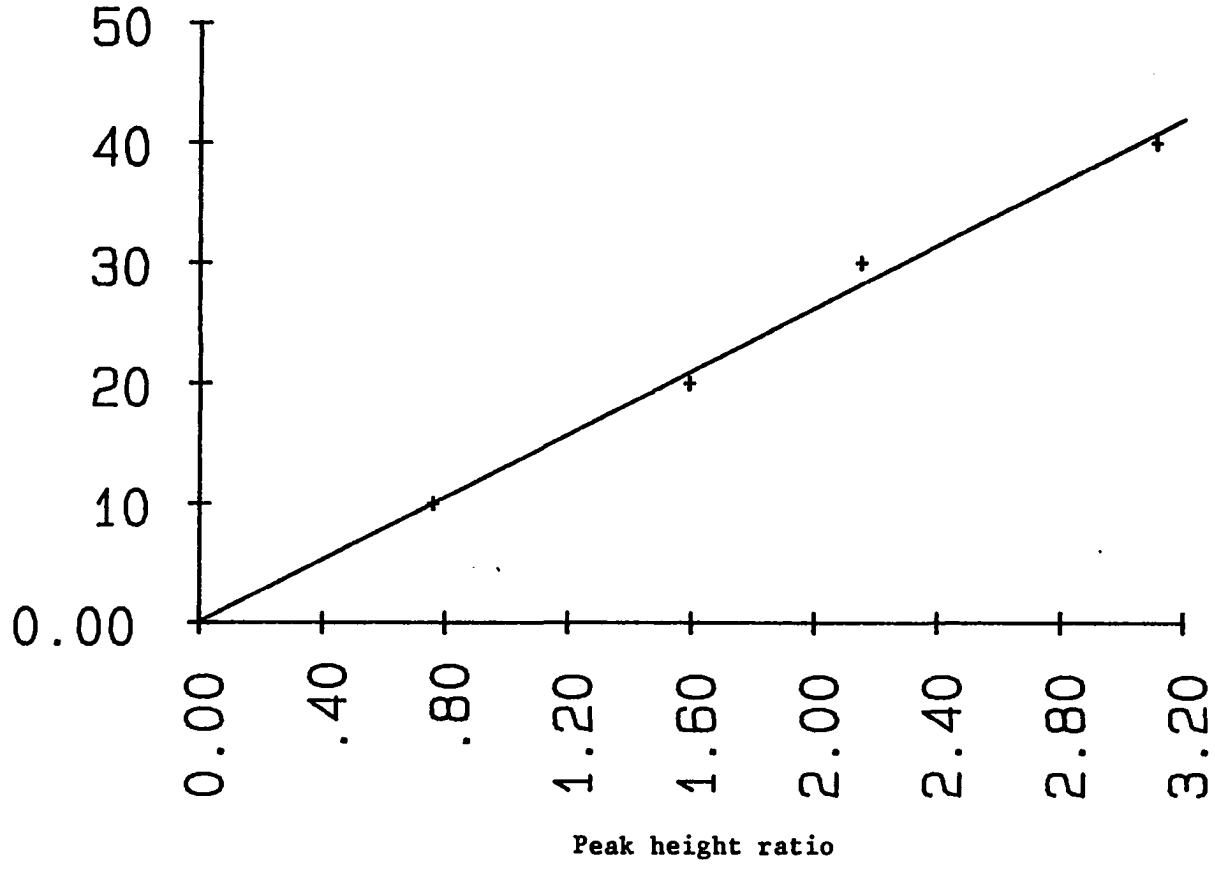

Figure 4-5 Calibration curve for the determination of dolomite by X-ray diffraction

Reproduced with permission of the copyright owner. Further reproduction prohibited without permission.

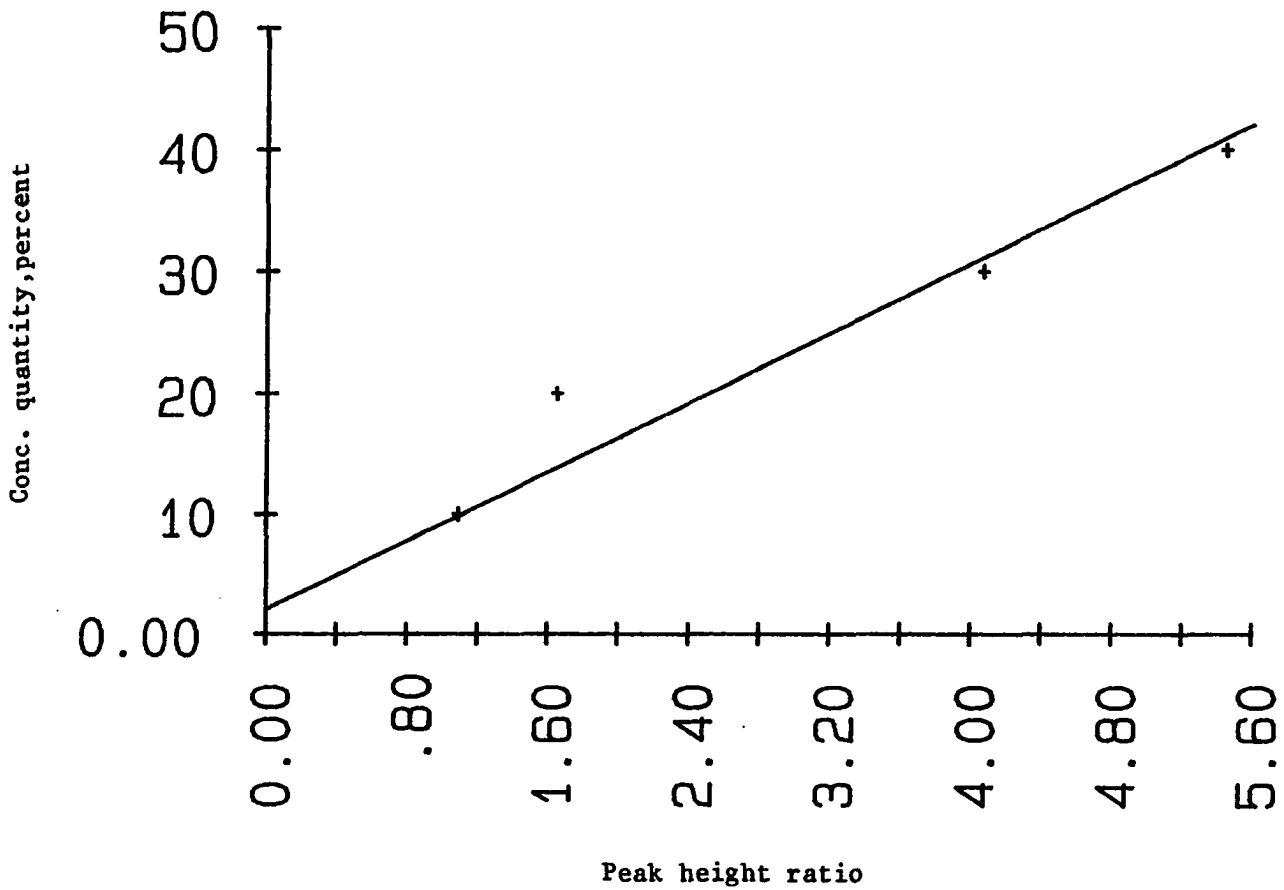

Figure 4-6 Calibration curve for the determination of siderite by X-ray diffraction

Identical setting of x-ray diffractometer and recorder are used for samples and standards. Percentages of the minerals in the sample are obtained by referring directly to their respective calibration curves using internal standard to sample peakheight ratios.

II) Infrared spectrographic determination of kaolinite

Procedures decribed by O'Gorman and Walker (1972) and Gong and Suhr (personal comm.) were used. Kaolinite used for the preparation of standards was pulverized and the fine fraction isolated by sedimentation. LTA samples were pulverized in an agate mortor wetted with ethanol. A 1 mg sample or standard was mixed with 200 mg of KBr and pelletized in an evacuated die with pressure maintained at 9 tons/sq. inch for 30 seconds. The pellets were scanned using a Perkin-Elmer model 467 double beam grating infrared spectrophotometer. Kaolinite is determined using the 910 cm-1 peak. Standard curves were drawn of absorbance vs concentration of kaolinite,and these gave a straight line relationship (Fig. 4-7). The baseline is obtained by connecting the background lows on either side of the peak by a straight line. Absorbance A is calculated as follows from the transmittance spectrum:

Reproduced with permission of the copyright owner. Further reproduction prohibited without permission.

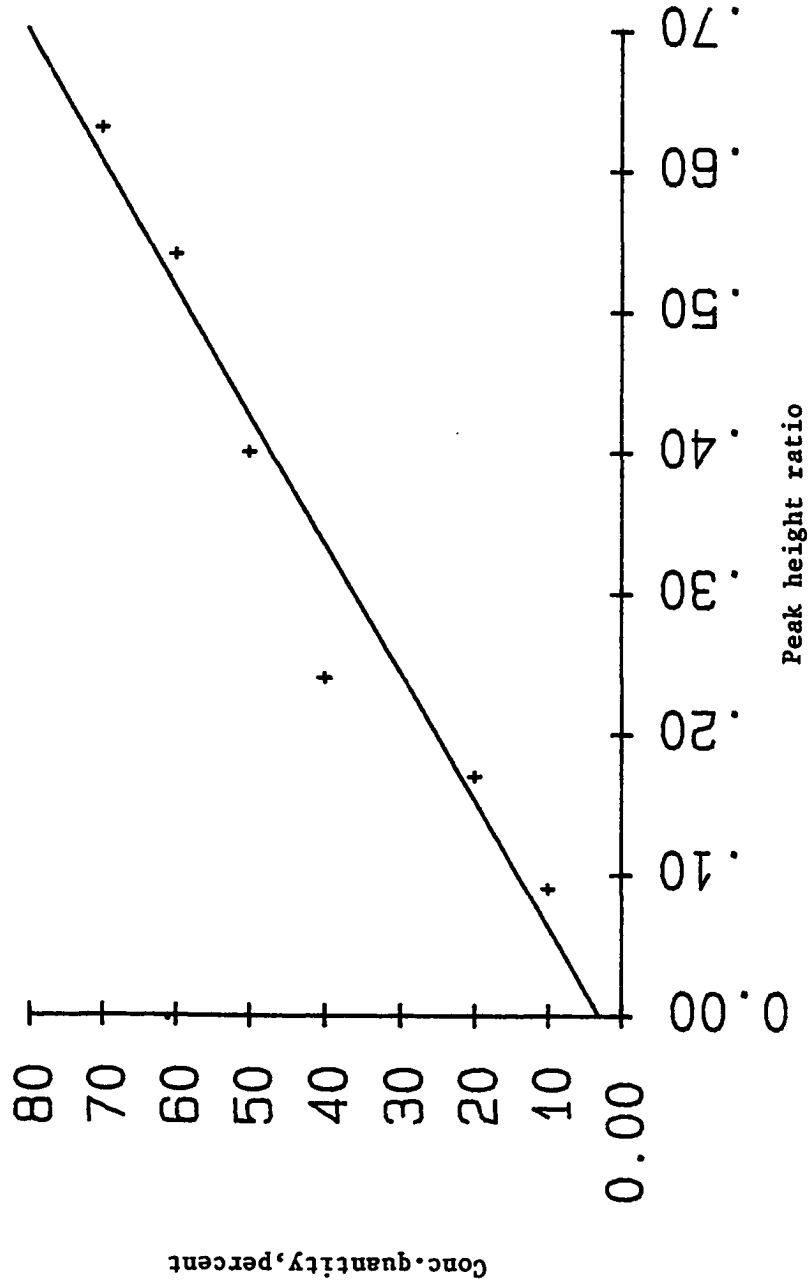

Figure 4-7 Calibration curve for the determination of kaolinite by infrared spectrometry analysis

Reproduced with permission of the copyright owner. Further reproduction prohibited without permission.

A=-log t=-log (reading at peak)/(reading at baseline at same wavelength as peak)

The "total other clays" (i.e. montmorillonite and illite and mixed layer clays) is calculated from mineralogical and chemical analysis (Gong and Suhr, per. comm.) as 2 times the remaining SiO_2, calculated as follows:

SiO_2 remaining = SiO_2 in MTA - [(kaolinite x 0.465) + (plagioclase x 0.687)
+ quartz]

Total other clays = SiO_2 remaining x 2

Also

Al_2O_3 remaining in = [(%MTA/%LTA) x (% Al_2O_3 in MTA)]

Total other clays = Al_2O_3 remaining x 4

In cases where the above two numbers do not agree, the mean of the two is used. Disagreement between the amounts of clays estimated from the remaining Al_2O_3 and SiO_2 is discussed in Gong's personal comm. (1977)

The mineralogy of the coals is shown in tables 5-7 to 5-12. Clay minerals are by far the most abundant in the samples.

Reproduced with permission of the copyright owner. Further reproduction prohibited without permission.

C) Maceral groups and microlithotypes study

I) Sample pellet preparation

Procedures outlined by ASTM (D2787-72, D2798-72, D2799-72) were followed. Fifty grams of minus 20 mesh coal was kneaded with enough epoxy resin to wet the grains, and briquetted in 1 inch diameter moulds with a hydraulic press at 4000 to 5000 PSI. The briquets were polished using a Buehler Automet, beginning with a 30 micron metal bonded diamond lap followed by Linde A (0.3 micron) and Linde B (0.05 micron) alumium oxide suspensions.

II) Maceral-microlithotype analysis

The combined maceral-microlithotype analysis method is recommended in Stach's Textbook of Coal Petrology (1982, 3rd ed.). This combined analysis not only provides the concentrations of microlithotypes and maceral groups, but also furnishes additional information on the mean maceral composition of the microlithotypes. This implies that maceral associations have to be considered in the maceral analyses. The point to be assessed in terms of maceral identity is at the centre of a graticule pattern. For the microlithotype analysis, Kotter's 20 point graticule was replaced by a square graticule having the same area

Reproduced with permission of the copyright owner. Further reproduction prohibited without permission.

and number of points with length on edge of 50u. Points are not counted unless at least 10 intersections of the graticule fall within a coal particle, but certain conventions are necessary to ensure that the combined analyses lead to the same results as those obtained by separate analyses by macerals and microlithotypes.

1) If the grain size is 30 microns or smaller the point can be situated on a maceral although fewer than 10 intersections fall inside the coal particle. In the maceral analysis such a point is counted; in analysis by microlithotypes it is disregarded, and in the combined analysis it is classified as an "isolated" maceral.

2) When the point is situated on a maceral without 10 intersections falling inside the coal particle, it is classified as a "maceral near the boundary" of the particle.

3) If more than 10 intersections are situated on a coal particle, whereas the reference point is not, it is classified as an "observed microlithotype".

Table 4-2 gives the categories of associated macerals which are distinguished in the combined analysis in its simplest form. In such a case one records only associations of maceral groups with other maceral groups and the carbominerites.

Reproduced with permission of the copyright owner. Further reproduction prohibited without permission.

Table 4-2 Categories of association for the simplest version of a combined analysis

No.	Composition of the associations
1	Vitrinite
2	Vitrinite at the boundary of the particle
3	Isolated vitrinite equal or less than 30 microns
4	Vitrinite in clarite
5	Vitrinite in trimacerite
6	Vitrinite in vitrinertite
7	Exinite
8	Exinite at the boundary of the particle
9	Isolated exinite
10	Exinite in clarite
11	Exinite in trimacerite
12	Exinite in durite
13	Inertinite
14	Inertinite at the boundary of the particle
15	Isolated inertinite
16	Inertinite in vitrinertite
17	Inertinite in trimacerite
18	Inertinite in durite
19	Minerals+dirt (isolated and at the boundary of a particle)
20	V,E,I + minerals (carbominerite)
21	Minerals + V,E,I (carbominerite)
22	Observed microlithotypes (observed carbominerite)

(Stach, 1983)

Reproduced with permission of the copyright owner. Further reproduction prohibited without permission.

For combined analysis 1000 points were counted on coal; in order to measure this number of points, a point-to-point and line-to-line distance of 0.4 to 0.5 mm on a polished section of 4 cm^2 is required, providing the ratio between the coal and the embedding material is at least 3:2.

The number of points counted is converted to percentages by volume and the values are given in whole numbers. For quick assessment of results a standard form was used to record analyses of maceral or maceral groups, and of microlithotypes, and to determine the maceral composition of the different microlithotypes. Figure 4-8 shows such a standard form which is confined to maceral groups, microlithotypes and carbominerites. In table 4-3 are listed the analytical values derived from the example of Figure 4-8. In calculating the composition of the coal sample by maceral groups, category 5("observed microlithotypes") is disregarded; in the calculation of the composition by microlithotypes categories a) and j) ("isolated macerals" and "macerals at the boundary of the particle") are neglected.

Reproduced with permission of the copyright owner. Further reproduction prohibited without permission.

Table 4-3 Results of the combined analysis

Maceral groups	Vol%	Microlithotypes	Vol.%	V	E	I	M
Vitrinite	66	Vitrite	34	100			
Exinite	9	Liptite	<1	100			
Inertinite	24	Inertite	7			100	-
		clarite	14	85	15	-	-
Minerals	1	Durite	4		29	71	-
		Vitrinertite	15	64	-	36	<1
	100	Trimacerite	24	50	22	28	-
		Carbominerite + Mineral matter	1		20		80

(Stach, 1983)

Reproduced with permission of the copyright owner. Further reproduction prohibited without permission.

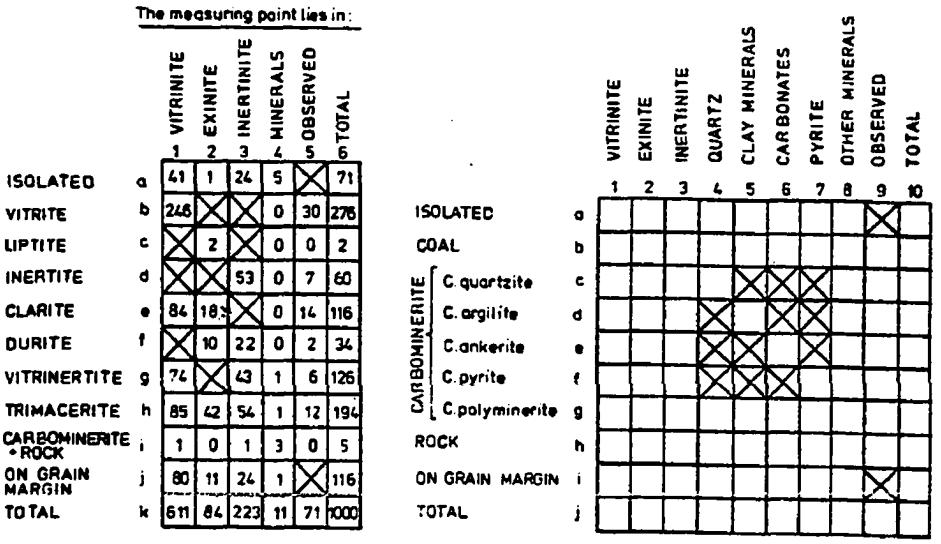

Figure 4-8 Standard form to record the results of the combined analysis: a) for maceral groups and microlithotypes; b) for maceral groups, minerals, coal and carbominerites.
(Stach, 1982)

Reproduced with permission of the copyright owner. Further reproduction prohibited without permission.

CHAPTER 5

RESULTS AND DISCUSSIONS

I) Maceral groups and Macrolithotypes

Densimetric fractions from float-sink separations of raw coals crushed to 1 1/2 inches and 14 mesh were used to determine the possibilities of concentrating petrographic constituents in coal washing processes. Since the float-sink separation were done at a relatively coarse size and the possibility of liberation of microlithotypes could be more pronounced than the macerals themselves. Petrological analyses were, therefore, done to determine both the concentration of macerals groups as well as microlithotypes. Analytical results are presented in Tables 5-1 to 5-6. In general, liptites were absent in all six coals studied, durite was only identified in two seams i.e., UA-149 from Johnson Creek and UA-152 from Long Ridge Mine and was only in a trace quantity. The principal microlithotypes in the coals were vitrite, inertite, clarite, vitrinertite and trimacerite. In general vitrite concentration was higher in lower density fractions as can be expected. Inertite was concentrated in higher density fractions, particulary for sample from NO. 7 bed coal from Cape Beaufort and No.3 bed coal sample from Healy. Both

Reproduced with permission of the copyright owner. Further reproduction prohibited without permission.

Reproduced with permission of the copyright owner. Further reproduction prohibited without permission.

Table-5-1

Maceral groups and microlithotypes distribution in the washing products from the No. 3 Bed Coal Sample (UA-130) Healy, Alaska

Concentration, Volume percent

Product	microlithotypes Mm*-free basis							maceral groups Mm-free basis			mineral matter Mm-contained basis	
	Vitrite	Liptite	Inertite	Clarite	Durite	Vitrinertite	Trimacerite	Vitrinite	Exinite	Inertinite	Carbominerite+Minerals	Minerals
Float-Sink Size 1-1/2 inches x 100 Mesh												
Float-1.3	40	0	2	38	0	6	14	80	11	9	2	2
1.3 -1.4	55	0	2	30	0	6	7	88	7	5	1	1
1.4 -1.6	31	0	1	61	0	1	6	77	19	4	7	2
1.6 -Sink	50	0	25	25	0	0	0	96	1	3	96	37
Float-Sink Size 14 Mesh x 0												
Float-1.3	34	0	3	41	0	6	16	78	15	7	2	1
1.3 -1.4	33	0	4	41	0	8	14	81	10	9	2	2
1.4 -1.6	22	0	21	28	0	16	13	56	7	37	8	2
1.6 -Sink	60	0	20	20	0	0	0	94	2	4	95	50

*Mineral matter

Reproduced with permission of the copyright owner. Further reproduction prohibited without permission.

Table-5-2

Maceral groups and microlithotypes distribution in the washing products from an Uncorrelated Bed Coal Sample (UA-136) Chignik Mine, Alaska

Concentration, Volume percent

Product	microlithotypes Mm*-free basis							maceral groups Mm-free basis			mineral matter Mm-contained basis	
	Vitrite	Liptite	Inertite	Clarite	Durite	Vitrinertite	Trimacerite	Vitrinite	Exinite	Inertinite	Carbominerite+Minerals	Minerals
Float-Sink Size 1-1/2 inches x 100 Mesh												
Float-1.3	66	0	1	17	0	12	4	94	2	4	8	1
1.3 -1.4	63	0	1	10	0	11	15	93	2	5	7	1
1.4 -1.6	70	0	1	15	0	9	5	95	3	2	14	4
1.6 -Sink	67	0	2	13	0	13	5	93	2	5	36	13
Float-Sink Size 14 Mesh x 0												
Float-1.3	15	0	0	13	0	2	70	88	7	5	0	0
1.3 -1.4	24	0	1	20	0	6	49	88	5	7	0	0
1.4 -1.6	53	0	0	33	0	8	6	91	7	2	10	2
1.6 -Sink	29	0	1	29	0	9	31	86	12	2	42	15

*Mineral matter

Reproduced with permission of the copyright owner. Further reproduction prohibited without permission.

Table-5-3

Maceral groups and microlithotypes distribution in the washing products from the No.7 Bed Coal Sample (UA-139) Chignik Mine, Alaska

Concentration, Volume percent

Product	microlithotypes Mm*-free basis							maceral groups Mm-free basis			mineral matter Mm-contained basis	
	Vitrite	Liptite	Inertite	Clarite	Durite	Vitrinertite	Trimacerite	Vitrinite	Exinite	Inertinite	Carbominerite+Minerals	Minerals
Float-Sink Size 1-1/2 inches x 100 Mesh												
Float-1.3	0	0	0	0	0	0	0	0	0	0	0	0
1.3 -1.4	54	0	1	27	0	11	7	87	6	7	1	0
1.4 -1.6	23	0	13	13	0	40	11	64	5	31		
1.6 -Sink	21	0	18	15	0	34	12	59	6	35	32	29
Float-Sink Size 14 Mesh x 0												
Float-1.3	0	0	0	0	0	0	0	0	0	0	0	0
1.3 -1.4	57	0	5	20	0	25	3	84	5	11	1	1
1.4 -1.6	30	0	19	6	0	38	7	61	3	36	1	1
1.6 -Sink	9	0	36	0	0	52	3	48	1	51	36	21

*Mineral matter

Reproduced with permission of the copyright owner. Further reproduction prohibited without permission.

Table-5-4

Maceral groups and microlithotypes distribution in the washing products from the No.5 Bed Coal Sample (UA-147) Chignik Mine, Alaska

Concentration, Volume percent

Product	microlithotypes Mm*-free basis						maceral groups Mm-free basis			mineral matter Mm-contained basis	
	Vitrite	Liptite	Inertite	Clarite	Durite	Vitrinertite	Trimacerite	Vitrinite	Exinite	Inertinite	Carbominerite+Minerals	Minerals
Float-Sink Size 1-1/2 inches x 100 Mesh												
Float-1.3	75	0	0	23	0	1	1	95	4	1	0	0
1.3 -1.4	73	0	0	22	1	2	1	96	3	1	2	1
1.4 -1.6	73	0	0	25	0	1	1	96	4	0	12	3
1.6 -Sink	62	0	0	38	0	0	0	98	1	1	63	37
Float-Sink Size 14 Mesh x 0												
Float-1.3	72	0	1	22	1	3	1	93	5	2	3	0
1.3 -1.4	70	0	1	25	0	3	1	93	6	1	9	1
1.4 -1.6	58	0	0	38	0	3	1	96	4	0	16	0
1.6 -Sink	82	0	0	18	0	0	0	99	1	0	43	31

*Mineral matter

Reproduced with permission of the copyright owner. Further reproduction prohibited without permission.

Table-5-5

Maceral groups and microlithotypes distribution in the washing products from an uncorrelated Bed Coal Sample (UA-149) Johnson Creek, Alaska

Concentration, Volume percent

Product	microlithotypes Mm*-free basis							maceral groups Mm-free basis			mineral matter Mm-contained basis	
	Vitrite	Liptite	Inertite	Clarite	Durite	Vitrinertite	Trimacerite	Vitrinite	Exinite	Inertinite	Carbominerite+Minerals	Minerals
Float-Sink Size 1-1/2 inches x 100 Mesh												
Float-1.3	51	0	11	25	1	7	5	75	8	17	5	0
1.3 -1.4	27	0	10	40	6	9	8	71	9	20	2	0
1.4 -1.6	76	0	3	9	0	11	1	92	2	6	10	2
1.6 -Sink	66	0	0	34	0	0	0	86	3	11	75	37
Float-Sink Size 14 Mesh x 0												
Float-1.3	71	0	0	17	1	6	5	93	4	3	4	0
1.3 -1.4	66	0	1	22	0	5	6	92	4	4	8	1
1.4 -1.6	33	0	2	54	0	3	8	83	14	3	3	2
1.6 -Sink	not examined											

*Mineral matter

Reproduced with permission of the copyright owner. Further reproduction prohibited without permission.

Table-5-6

Maceral groups and microlithotypes distribution in the washing products from Green Bed Coal Sample (UA-152) Long Ridge Mine, Beluga, Alaska

Concentration, Volume percent

Product	microlithotypes Mm*-free basis							maceral groups Mm-free basis			mineral matter Mm-contained basis	
	Vitrite	Liptite	Inertite	Clarite	Durite	Vitrinertite	Trimacerite	Vitrinite	Exinite	Inertinite	Carbominerite+Minerals	Minerals
Float-Sink Size 1-1/2 inches x 100 Mesh												
Float-1.3	69	0	0	22	0	5	4	92	4	4	22	2
1.3 -1.4	67	0	1	24	0	4	4	93	5	2	24	1
1.4 -1.6	63	0	1	32	0	1	2	88	11	1	41	6
1.6 -Sink	67	0	0	33	0	0	0	98	1	1	88	56
Float-Sink Size 14 Mesh x 0												
Float-1.3	48	0	10	26	0	8	8	76	7	17	16	1
1.3 -1.4	51	0	11	23	1	8	6	79	5	16	16	1
1.4 -1.6	53	0	6	22	1	14	4	81	5	14	19	4
1.6 -Sink	49	0	7	23	0	18	3	77	7	16	33	17

*Mineral matter

coals showed improved liberation of inertite when crushed to 14 mesh. For example, the sample from Cape Beaufort 1.6 sinks from 14 mesh by 0 coal sample contained 36% inertite and 52% vitrinertite showing the liberation of those microlithotypes due to crushing. It proves that possibilities of petrographic beneficiation of samples exist for concentrating coals to obtain highly reactive macerals for coking or liquefaction process. With the exception of sample from Johnson Creek, all other samples showed a generally higher concentration of clarite in lower density fractions. UA-149 from Johnson Creek, however, showed higher concentration in 1.6 sinks possibly due to the association of clarite with inorganic material. Vitrinertite however is generally concentrated in the intermediate density fractions for 1 1/2 inches size material and was concentrated in 1.6 sinks for 14 mesh material showing the liberation of this microlithotypes due to crushing. Only the sample from Chignik Mine showed a significantly higher concentration of trimacerite and the concentrations are generally high in the lower density fractions although 14 mesh by 0 material showed 30% trimacerite in 1.6 sinks. The coal sample from Healy, UA-130, showed high concentrations of trimacerite in the low density fractions and the 1.6 sinks did not contain any trimacerite. Among maceral

Reproduced with permission of the copyright owner. Further reproduction prohibited without permission.

groups, only sample from Cape Beaufort showed very significant concentration of vitrinite in the low density fractions while eliminating inerinite in the higher density fractions. The 1 1/2 inches by 100 mesh material contained 35% inertinite in 1.6 sinks, when crushed to 14 mesh the 1.6 sinks contained 51% inertinite showing that the sample from Cape Beaufort can be beneficiated to concentrate reactive macerals. The low density fractions contained very low concentration of carbominerite and minerals, since much of the ash forming impurities are contained as inherent ash not recognizable under the microscope, whereas 1.6 sinks containing majority of the ash as mineral matter accounted for the high concentration of carbominerite and minerals.

Influence of washing on the composition of coal ash and on the mineral matter

II) Major oxides

All samples with exception of sample UA 147 from Evan Jones showed a similar trend of concentration of major oxides (Table 5-7 to 5-12) with changing density. The compounds SiO_2, Al_2O_3 and K_2O generally showed a trend of increasing concentrations with increasing density. This is due to the fact that SiO_2 and Al_2O_3 are generally present as clay minerals or free quartz, and k_2O is associated with illite, which are therefore highly

Reproduced with permission of the copyright owner. Further reproduction prohibited without permission.

Reproduced with permission of the copyright owner. Further reproduction prohibited without permission.

Table-5-7

Distribution of major oxides in the ash of washability products from the No.3 Bed Coal Sample (UA-130) Usibelli Coal Mine. Healy, Alaska

Raw Coal Bed Moisture = 24.54

Product	Ash%	SiO_2	Al_2O_3	Fe_2O_3	MgO	CaO	K_2O	Na_2O	TiO_2	MnO	P_2O_5	SO_3
					in the Ash of Actual Product, percent							
					Float-Sink Size 1-1/2 inches x 100 Mesh							
Float-1.3	4.63	7.10	7.40	10.20	6.40	58.90	0.01	0.12	0.34	2.98	0.94	5.80
1.3 -1.4	6.81	21.20	12.20	10.40	4.79	43.80	0.34	0.13	0.72	2.28	0.51	3.84
1.4 -1.6	13.44	54.80	22.10	4.30	1.95	11.40	1.82	0.21	1.06	0.76	0.07	1.63
1.6 -Sink	68.75	71.50	20.40	1.40	0.70	2.00	1.83	0.12	1.60	0.23	0.12	0.08
Raw coal	12.51	48.20	15.40	6.50	2.83	19.70	1.21	0.29	0.90	1.23	0.10	3.93
					Float-Sink Size 14 Mesh x 0							
Float-1.3	4.60	17.70	11.00	7.30	6.77	48.20	0.08	0.14	0.50	2.57	0.14	5.73
1.3 -1.4	9.12	23.20	12.10	10.30	4.55	42.40	0.28	0.13	0.83	2.33	0.43	3.58
1.4 -1.6	17.87	46.90	19.80	8.10	2.42	16.50	1.32	0.13	0.97	0.97	0.10	2.84
1.6 -Sink	70.92	72.20	17.90	3.50	0.63	1.60	1.87	0.11	1.35	0.47	0.25	0.10

All results are on a Moisture Free Basis.

Reproduced with permission of the copyright owner. Further reproduction prohibited without permission.

Table-5-8

Distribution of major oxides in the ash of washability products from an Uncorrelated Bed Coal Sample (UA-136) Chignik Mine, Chignik, Alaska

Raw Coal Bed Moisture = 6.66

	in the Ash of Actual Product, percent											
Product	Ash%	SiO_2	Al_2O_3	Fe_2O_3	MgO	CaO	K_2O	Na_2O	TiO_2	MnO	P_2O_5	SO_3
					Float-Sink Size 1-1/2 inches x 100 Mesh							
Float-1.3	4.06	19.60	20.90	16.20	7.79	15.20	0.17	0.27	1.67	1.24	0.78	16.50
1.3 -1.4	7.65	41.70	28.20	9.00	3.76	6.80	0.70	0.21	1.88	0.59	0.43	6.90
1.4 -1.6	20.49	47.30	28.00	7.30	1.75	6.20	0.73	0.18	1.16	0.39	1.37	5.90
1.6 -Sink	59.53	56.60	30.80	3.80	0.92	2.80	1.17	0.25	1.17	0.27	0.06	2.40
Raw coal	36.18	54.20	29.70	7.40	1.22	3.80	1.13	0.18	1.17	0.23	0.06	3.20
					Float-Sink Size 14 Mesh x 0							
Float-1.3	2.75	16.20	23.60	10.10	14.30	15.30	0.06	0.26	1.34	0.97	0.28	17.80
1.3 -1.4	8.00	29.10	23.10	13.60	5.40	12.50	0.21	0.62	1.21	0.86	0.42	13.60
1.4 -1.6	20.69	50.70	30.30	6.80	1.40	3.10	0.87	0.23	1.63	0.36	1.51	3.30
1.6 -Sink	59.34	55.80	30.20	4.40	0.92	3.40	1.15	0.17	1.05	0.31	0.05	1.20

All results are on a Moisture Free Basis.

Reproduced with permission of the copyright owner. Further reproduction prohibited without permission.

Table-5-9

Distribution of major oxides in the ash of washability products from the No. 7 Bed Coal Sample (UA-139) Cape Beaufort, Alaska

Raw Coal Bed Moisture = 11.25

Product	Ash%	SiO_2	Al_2O_3	Fe_2O_3	MgO	CaO	K_2O	Na_2O	TiO_2	MnO	P_2O_5	SO_3
					Actual Product, percent							
					Float-Sink Size 1-1/2 inches x 100 Mesh							
Float-1.3	0.00	0.00	0.00	0.00	0.00	0.00	0.00	0.00	0.00	0.00	0.00	0.00
1.3 -1.4	5.32	31.50	18.70	5.34	5.20	7.40	0.99	7.73	0.72	0.84	2.91	9.57
1.4 -1.6	12.20	50.20	25.10	3.15	3.00	9.67	0.85	3.52	1.01	0.43	0.44	2.59
1.6 -Sink	60.01	66.10	24.40	1.34	1.45	1.44	1.36	2.31	0.70	0.22	0.62	0.14
Raw coal		60.10	23.80	2.26	2.28	4.52	1.16	3.19	0.84	0.30	0.22	1.23
					Float-Sink Size 14 Mesh x 0							
Float-1.3	0.00	0.00	0.00	0.00	0.00	0.00	0.00	0.00	0.00	0.00	0.00	0.00
1.3 -1.4	4.90	31.00	18.40	5.08	4.32	17.60	1.03	8.24	1.09	1.03	2.40	9.75
1.4 -1.6	9.73	45.60	23.80	3.24	3.24	11.20	0.81	3.97	1.11	0.48	0.57	6.06
1.6 -Sink	50.42	64.70	24.40	1.64	1.85	2.47	1.25	2.51	0.71	0.23	0.12	0.12

All results are on a Moisture Free Basis.

Reproduced with permission of the copyright owner. Further reproduction prohibited without permission.

Table-5-10

Distribution of major oxides in the ash of washability products from the No. 5 Bed Coal Sample (UA-147) Evan Jones Mine, Matanuska, Alaska

Raw Coal Bed Moisture = 4.82

	in the Ash of Actual Product, percent											
Product	Ash%	SiO_2	Al_2O_3	Fe_2O_3	MgO	CaO	K_2O	Na_2O	TiO_2	MnO	P_2O_5	SO_3
				Float-Sink Size 1-1/2 inches x 100 Mesh								
Float-1.3	2.92	55.40	30.20	6.30	1.05	2.16	0.75	0.22	0.80	0.58	0.20	2.28
1.3 -1.4	10.09	54.60	32.90	3.31	1.47	1.36	1.77	0.41	2.20	0.32	1.24	0.40
1.4 -1.6	24.12	59.60	30.40	2.74	1.45	0.45	2.41	0.52	1.72	0.29	0.43	0.00
1.6 -Sink	61.04	55.30	26.00	9.10	2.28	1.55	2.25	0.40	1.10	1.20	0.75	0.06
Raw coal	35.94	55.50	27.00	7.13	2.44	1.99	2.26	0.19	1.27	0.88	1.18	0.18
				Float-Sink Size 14 Mesh x 0								
Float-1.3	2.96	36.20	35.40	8.34	3.10	5.87	0.87	1.82	2.91	0.34	2.45	2.67
1.3 -1.4	5.63	48.00	32.60	4.61	2.15	3.15	1.65	0.89	3.88	0.21	1.67	1.23
1.4 -1.6	22.60	56.40	28.60	4.73	2.06	1.64	2.32	0.20	1.82	0.46	1.12	0.60
1.6 -Sink	55.16	55.90	26.80	7.11	2.55	2.01	2.27	0.21	1.06	0.89	1.22	0.01

All results are on a Moisture Free Basis.

Reproduced with permission of the copyright owner. Further reproduction prohibited without permission.

Table-5-11

Distribution of major oxides in the ash of washability products from an Uncorrelated Bed Coal Sample (UA-149) Johnson Creek, Yentna Field, Alaska

Raw Coal Bed Moisture = 25.34

		in the Ash of Actual Product, percent									
Product	Ash%	SiO_2	Al_2O_3	Fe_2O_3	MgO	CaO	K_2O	Na_2O	TiO_2	MnO	P_2O_5	SO_3
					Float-Sink Size 1-1/2 inches x 100 Mesh							
Float-1.3	5.24	28.20	19.90	8.69	4.97	27.30	1.14	0.27	0.64	0.96	2.75	5.44
1.3 -1.4	10.78	43.00	23.50	5.12	3.44	15.80	1.79	0.37	0.91	0.65	2.98	2.70
1.4 -1.6	28.77	59.10	24.80	2.98	1.90	5.20	2.65	0.35	1.09	0.40	1.29	0.62
1.6 -Sink	64.21	64.00	22.00	6.14	1.51	1.20	2.61	0.73	0.97	0.63	0.42	0.21
Raw coal	13.67	47.70	22.90	6.20	2.92	12.60	2.00	0.33	0.91	0.71	1.72	2.41
					Float-Sink Size 14 Mesh x 0							
Float-1.3	4.87	25.00	20.20	9.03	5.74	29.90	0.89	0.35	0.60	0.96	1.85	5.63
1.3 -1.4	9.01	39.80	22.40	6.08	4.09	19.20	1.60	0.28	0.87	0.69	2.78	2.45
1.4 -1.6	23.78	55.50	24.80	3.93	2.25	7.60	2.45	0.24	1.06	0.48	1.71	0.21
1.6 -Sink	39.74	60.00	22.70	6.93	1.76	3.20	2.52	0.57	0.95	0.78	0.87	0.11

All results are on a Moisture Free Basis.

Reproduced with permission of the copyright owner. Further reproduction prohibited without permission.

Table-5-12

Distribution of major oxides in the ash of washability products from Green Bed Coal Sample (UA-152) Long Ridge Mine, Beluga Field, Alaska

Raw Coal Bed Moisture = 27.59

	in the Ash of Actual Product, percent											
Product	Ash%	SiO_2	Al_2O_3	Fe_2O_3	MgO	CaO	K_2O	Na_2O	TiO_2	MnO	P_2O_5	SO_3
					Float-Sink Size 1-1/2 inches x 100 Mesh							
Float-1.3	3.55	13.30	16.70	11.60	7.65	44.10	0.24	0.30	0.48	0.89	2.10	2.95
1.3 -1.4	7.16	33.40	22.80	9.40	4.89	24.10	1.02	0.32	0.74	0.72	0.19	2.56
1.4 -1.6	22.06	50.60	31.60	3.30	1.66	6.50	1.24	0.24	0.96	0.34	0.10	0.56
1.6 -Sink	64.69	58.60	34.50	2.61	0.65	1.40	0.65	0.44	0.79	0.32	0.18	0.02
Raw coal	8.25	34.60	23.80	8.30	4.36	23.30	0.75	0.37	0.69	0.64	0.20	3.19
					Float-Sink Size 14 Mesh x 0							
Float-1.3	3.80	18.80	19.10	11.00	6.45	39.50	0.47	0.39	0.63	0.84	0.27	2.80
1.3 -1.4	7.39	34.10	24.00	7.60	4.66	25.00	0.95	0.33	0.77	0.60	0.23	2.05
1.4 -1.6	15.12	46.00	28.90	6.00	2.77	12.30	1.24	0.30	0.85	0.48	0.18	1.20
1.6 -Sink	56.94	56.80	30.40	6.80	1.01	2.20	0.79	0.48	0.88	0.66	0.22	0.03

All results are on a Moisture Free Basis.

concentrated in the higher density fractions. The two other compounds MgO, CaO show higher concentrations in the low density fraction and the concentrations decrease with increasing density. Most of the calcium is present inThelow density fraction in a chealated form. The sample from Usibelli Coal Mine UA 130 showed as high as 58.9% CaO in 1.3 float fraction and the concentration reduces down to 2% in 1.6 sink fraction. Similarly Fe_2O_3 showed high concentrations in these samples in the lower density fractions with concentration decreasing with increase in density. The MnO showed a trend similar to Fe_2O_3 as manganese is expected to behave similar to iron oxides. The two elements phosphorus and sulfur similarly show high concentrations in the lower density fractions. Sulfur in many of these coals is present as organic Sulfur and is retained in the ash by calcium present in the coal as calcium sulfate. The form in which phosphorous is present in these coals has not been established. Concentration of sodium is generally low in Alaskan coals as these coals are nonmarine and the coal ashes did not show any specific trend of concentration with the density. The sample from Evan Jones however showed entirely different behavior. Bulk of the ash is composed of SiO_2 and Al_2O_3 and various density densimetric fraction, therefore, did not show any trend in the variation of SiO_2 or Al_2O_3. Fe_2O_3,

Reproduced with permission of the copyright owner. Further reproduction prohibited without permission.

CaO and MnO showed increase in concentration with decreasing density with exception of 1.6 sinks. The 1.6 sinks however showed highest concentrations of Fe_2O_3, CaO and MnO, due to the fact of that much of Fe_2O_3, CaO in 1.6 sinks are present as carbonates as shown by XRD analyses of low temperature ashes (Tables 5-13 to 5-18). K_2O however showed increase concentration with increasing density as was the case with the other five samples.

III) Mineral matter

Distribution of mineral in the LTA is presented in Tables 5-13 to 5-18. In general, quartz and kaolinite showed increasing concentration with increased density and showed the liberation and separation effect of washability in all six coals. The concentration of plagioclase in the highest density also showed the fact of separation effect of washability. A small amount of carbonates is detected in most samples. Calcite and dolomite showed that concentration is increased with increasing density when the sample is crushed to finer size except in the sample of Johnson Creek and Long Ridge Mine. This proved the possibility of liberation of minerals due to crushing and separation by washing. Siderite showed to be concentrated in the highest density fractions in most samples. This showed that siderite is easily separated.

Reproduced with permission of the copyright owner. Further reproduction prohibited without permission.

Reproduced with permission of the copyright owner. Further reproduction prohibited without permission.

Table-5-13

Mineral distribution in the LTA of washing products from the No.3 Bed Coal Sample (UA-130) Usibilli Coal Mine ,Healy, Alaska

Product	Wt percent in product *LTA	Wt percent in LTA Quartz	Kaollinite	Calcite	Dolomite	Siderite	Plagioclase	other clays
			Float-Sink Size 1-1/2 inches x 100 Mesh					
Float-1.3	7.29	3	4	0	0	0	0	11
1.3 -1.4	14.83	5	7	0	0	0	0	27
1.4 -1.6	34.97	22	21	0	0	0	0	37
1.6 -Sink	68.75	47	18	0	0	2	5	22
Raw coal		19	14	0	0	1	3	31
			Float-Sink Size 14 Mesh x 0					
Float-1.3	8.98	4	4	0	0	0	0	24
1.3 -1.4	13.42	7	6	0	0	0	0	30
1.4 -1.6	30.63	10	21	0	0	0	0	40
1.6 -Sink	79.44	54	21	0	0	2	4	19

*Moisture Free Basis.

Reproduced with permission of the copyright owner. Further reproduction prohibited without permission.

Table-5-14

Mineral distribution in the LTA of washing products from an Uncorrelated Bed Coal Sample (UA-136) Chignik Mine, Chignik, Alaska

Product	Wt percent in product *LTA	Wt percent in LTA Quartz	Kaollinite	Calcite	Dolomite	Siderite	Plagioclase	other clays
				Float-Sink Size 1-1/2 inches x 100 Mesh				
Float-1.3	6.01	3	16	4	7	0	0	34
1.3 -1.4	9.55	5	17	7	7	0	0	59
1.4 -1.6	24.32	14	33	6	3	0	0	34
1.6 -Sink	67.86	25	48	3	1	0	0	17
Raw coal		12	34	3	2	0	0	38
				Float-Sink Size 14 Mesh x 0				
Float-1.3	4.84	3	13	0	7	0	0	34
1.3 -1.4	10.98	7	31	2	4	0	0	19
1.4 -1.6	22.84	15	54	2	2	0	0	14
1.6 -Sink	68.99	26	40	4	1	0	0	22

*Moisture Free Basis.

Reproduced with permission of the copyright owner. Further reproduction prohibited without permission.

Table-5-15

Mineral distribution in the LTA of washing products from the No. 7 Bed Coal Sample (UA-139) Cape Beaufort, Alaska

Product	Wt percent in product *LTA	Wt percent in LTA Quartz	Kaollinite	Calcite	Dolomite	Siderite	Plagioclase	other clays
				Float-Sink Size 1-1/2 inches x 100 Mesh				
Float-1.3	0.00	0	0	0	0	0	0	0
1.3 -1.4	8.79	3	8	3	1	2	0	50
1.4 -1.6	16.33	7	19	1	2	0	0	56
1.6 -Sink	66.56	10	23	0	1	0	3	60
Raw coal		10	22	1	2	0	3	56
				Float-Sink Size 14 Mesh x 0				
Float-1.3	0.00	0	0	0	0	0	0	0
1.3 -1.4	6.93	2	9	2	0	0	0	48
1.4 -1.6	13.04	7	19	2	2	1	0	54
1.6 -Sink	56.45	9	14	0	1	0	2	74

*Moisture Free Basis.

Reproduced with permission of the copyright owner. Further reproduction prohibited without permission.

Table-5-16

Mineral distribution in the LTA of washing products from the No. 5 Bed Coal Sample (UA-147) Evan Johns Mine, Matanuska, Alaska

Product	Wt percent in product *LTA	Wt percent in LTA Quartz	Kaollinite	Calcite	Dolomite	Siderite	Plagioclase	other clays
				Float-Sink Size 1-1/2 inches x 100 Mesh				
Float-1.3	3.89	7	29	2	3	3	0	56
1.3 -1.4	12.37	14	43	0	2	2	0	32
1.4 -1.6	28.05	19	47	0	0	0	0	22
1.6 -Sink	71.34	17	43	0	0	4	0	20
Raw coal		12	39	0	2	2	0	30
				Float-Sink Size 14 Mesh x 0				
Float-1.3	3.45	3	20	0	0	0	0	59
1.3 -1.4	7.17	11	39	1	0	1	0	32
1.4 -1.6	24.27	14	29	1	2	2	0	39
1.6 -Sink	53.14	19	31	0	1	3	0	33

*Moisture Free Basis.

Reproduced with permission of the copyright owner. Further reproduction prohibited without permission.

Table-5-17

Mineral distribution in the LTA of washing products from an Uncorrelated Bed Coal Sample (UA-149) Johnson Creek, Yentna, Alaska

Product	Wt percent in product *LTA	Wt percent in LTA Quartz	Kaollinite	Calcite	Dolomite	Siderite	Plagioclase	other clays
			Float-Sink Size 1-1/2 inches x 100 Mesh					
Float-1.3	13.89	7	9	2	0	0	0	35
1.3 -1.4	22.35	8	15	0	0	0	0	45
1.4 -1.6	47.67	15	23	0	0	0	0	43
1.6 -Sink	77.40	27	18	0	0	2	0	38
Raw coal		9	14	0	0	1	0	47
			Float-Sink Size 14 Mesh x 0					
Float-1.3	8.00	4	8	2	0	1	0	34
1.3 -1.4	18.04	8	13	0	0	0	0	38
1.4 -1.6	18.18	16	18	0	0	0	0	37
1.6 -Sink	51.83	29	21	0	0	3	0	24

*Moisture Free Basis.

Reproduced with permission of the copyright owner. Further reproduction prohibited without permission.

Table-5-18

Mineral distribution in the LTA of washing products from Green Bed Coal Sample (UA-152) Long Ridge Mine, Beluga, Alaska

Product	Wt percent in product *LTA	Wt percent in LTA Quartz	Kaollinite	Calcite	Dolomite	Siderite	Plagioclase	other clays
			Float-Sink Size 1-1/2 inches x 100 Mesh					
Float-1.3	5.26	3	5	2	0	2	0	28
1.3 -1.4	14.12	5	15	0	0	2	0	38
1.4 -1.6	34.39	6	34	0	0	1	0	43
1.6 -Sink	80.72	10	47	0	0	1	3	30
Raw coal		6	19	0	0	2	0	35
			Float-Sink Size 14 Mesh x 0					
Float-1.3	5.45	2	7	1	0	1	0	35
1.3 -1.4	15.12	5	13	0	0	1	0	44
1.4 -1.6	24.95	7	25	0	0	2	0	45
1.6 -Sink		13	48	0	0	2	3	0

*Moisture Free Basis.

IV) Ash fusibility

The characteristics of ash fusion behavior are a result of complex reactions dictated by the chemical composition of the ash. Tables 5-19 to 5-24 present fusibility data for various float-sink fractions of the six samples under oxidizing and reducing atmospheres. Ash fusibility temperatures tend to decrease with decreasing in particle density. This is attributable to higher CaO concentrations in ashes of lower density fractions. Ash fusion temperatures tend to increase with increasing density fraction due to higher concentration of SiO_2 and Al_2O_3. Correlation between major oxides and initial deformation temperature were made for samples from Healy, Chignik and Johnson Creek for both reducing and oxidizing atmospheres. For each individual densimetric fraction, the ratio of SiO_2/Al_2O_3, K was calculated. The ratio showed an exponetial correlated regression when against the initial deformation temperature. The regression coefficient R^2 and the deviation between predicted temperature and observed temperature are listed in Tables 5-25 to 5-27 and is less than 70^oF. Another method of prediction is by multiple linear regression of concentrations of SiO_2, Al_2O_3, Fe_2O_3, CaO, MgO as related to the ash fusion temperature by Scholz (1965),

Reproduced with permission of the copyright owner. Further reproduction prohibited without permission.

Reproduced with permission of the copyright owner. Further reproduction prohibited without permission.

Table 5-19 Ash fusion temperature of washability products from the No.3 Bed Coal sample (UA-130) Healy, Alaska

	Initial deformation Temperature		Softening Temperature		Fluid Temperature	
	Oxi.	Red.	Oxi.	Red.	Oxi.	Red.
	Float-Sink Size 1-1/2 inches x 100 Mesh					
Float-1.3	2130	1910	x	x	x	x
1.3 -1.4	2230	2154	2414	2310	2480	2375
1.4 -1.6	2330	2287	2404	2370	2564	2492
1.6 -Sink	2512	2575	+2800	2785	+2800	+2800
Raw coal	2115	1980	2179	2094	2473	2190
	Float-Sink Size 14 Mesh x 0					
Float-1.3	2072	2083	2295	2226	2350	2369
1.3 -1.4	2080	2159	2395	2261	2405	2396
1.4 -1.6	2130	2162	2320	2240	2390	2430
1.6 -SinK	2402	2516	2704	2653	2787	+2800

Oxi.(Oxidizing atmosphere)
Red.(Reducing atmosphere)
x. cone condition not recognizable

Table 5-20 Ash fusion temperature of washability products from an Uncorrelated Bed coal sample (UA-136) Chignik Mine, Chignik, Alaska

	Initial deformation Temperature		Softening Temperature		Fluid Temperature	
	Oxi.	Red.	Oxi.	Red.	Oxi.	Red.
	Float-Sink Size 1-1/2 inches x 100 Mesh					
Float-1.3	2280	2034	X	2780	X	X
1.3 -1.4	2265	2270	2604	2433	2650	2570
1.4 -1.6	2593	2520	2745	2637	+2800	+2800
1.6 -SinK	+2800	2630	+2800	+2800	+2800	+2800
Raw coal	2730	2580	+2800	2755	+2800	+2800
	Float-Sink Size 14 Mesh x 0					
Float-1.3	2020	1990	x	2493	x	2557
1.3 -1.4	2230	2231	2450	2406	2530	+2800
1.4 -1.6	2400	2395	+2800	2754	+2800	+2800
1.6 -Sink	2620	2614	+2800	+2800	+2800	+2800

Oxi.(Oxidizing atmosphere)
Red.(Reducing atmosphere)
x. cone condition not recognizable

Reproduced with permission of the copyright owner. Further reproduction prohibited without permission.

Reproduced with permission of the copyright owner. Further reproduction prohibited without permission.

Table 5-21 Ash fusion temperature of washability products from the No.7 Bed Coal sample (UA-139) Cape Beaufort, Alaska

	Initial deformation Temperature		Softening Temperature		Fluid Temperature	
	Oxi.	Red.	Oxi.	Red.	Oxi.	Red.
	Float-Sink Size 1-1/2 inches x 100 Mesh					
Float-1.3	0	0	0	0	0	0
1.3 -1.4	2384	1970	2502	2033	2514	2056
1.4 -1.6	2350	2205	2424	2334	2475	2506
1.6 -Sink	2510	2298	2782	2663	+2809	2758
Raw coal	2253	2231	2435	2322	2549	2482
	Float-Sink Size 14 Mesh x 0					
Float-1.3	0	0	0	0	0	0
1.3 -1.4	2230	1855	2363	2013	2439	2058
1.4 -1.6	2280	2130	2476	2232	2492	2496
1.6 -Sink	2310	2230	2640	2530	2724	2650

Oxi.(Oxidizing atmosphere)
Red.(Reducing atmosphere)

Reproduced with permission of the copyright owner. Further reproduction prohibited without permission.

Table 5-22 Ash fusion temperature of washability products from an Uncorrelated Bed Coal sample (UA-147) Evan Johns Mine, Matanuska, Alaska

	Initial deformation Temperature		Softening Temperature		Fluid Temperature	
	Oxi.	Red.	Oxi.	Red.	Oxi.	Red.
	Float-Sink Size 1-1/2 inches x 100 Mesh					
Float-1.3	2250	2374	2670	2544	2753	2800
1.3 -1.4	2710	2555	+2800	+2800	+2800	+2800
1.4 -1.6	+2800	2400	+2800	+2800	+2800	+2800
1.6 -Sink	2655	2422	+2800	2574	+2800	2732
Raw coal	2645	2330	2749	2648	+2800	2767
	Float-Sink Size 14 Mesh x 0					
Float-1.3	2260	1920	2364	2530	2748	2779
1.3 -1.4	2495	2380	+2800	2776	+2800	+2800
1.4 -1.6	2440	2310	+2800	2798	+2800	+2800
1.6 -Sink	2570	2410	2725	2604	+2800	2700

Oxi.(Oxidizing atmosphere)
Red.(Reducing atmosphere)

Reproduced with permission of the copyright owner. Further reproduction prohibited without permission.

Table 5-23 Ash fusion temperature of washability products from an Uncorrelated Bed Coal sample (UA-149) Johnson Creek, Yentna, Alaska

	Initial deformation Temperature		Softening Temperature		Fluid Temperature	
	Oxi.	Red.	Oxi.	Red.	Oxi.	Red.
	Float-Sink Size 1-1/2 inches x 100 Mesh					
Float-1.3	2174	1945	2228	2056	2280	2154
1.3 -1.4	2190	2016	2417	2437	2485	2510
1.4 -1.6	2307	2080	2575	2457	2640	2600
1.6 -Sink	2520	2222	2697	2580	2734	2681
Raw coal	2155	1948	2370	2291	2480	2403
	Float-Sink Size 14 Mesh x 0					
Float-1.3	1985	1935	2390	x	2524	x
1.3 -1.4	2130	2050	2190	2270	2495	+2800
1.4 -1.6	2280	1985	2445	2290	2530	+2800
1.6 -Sink	2350	2220	2560	2411	2676	2577

Oxi.(Oxidizing atmosphere)
Red.(Reducing atmosphere)
x. cone condition not recognizable

Reproduced with permission of the copyright owner. Further reproduction prohibited without permission.

Table 5-24 Ash fusion temperature of washability products from Green Bed Coal sample (UA-152) Long Ridge Mine, Beluga, Alaska

	Initial deformation Temperature		Softening Temperature		Fluid Temperature	
	Oxi.	Red.	Oxi.	Red.	Oxi.	Red.
	Float-Sink Size 1-1/2 inches x 100 Mesh					
Float-1.3	2120	2010	x	x	x	x
1.3 -1.4	2268	2068	2305	2138	2368	2210
1.4 -1.6	2750	2580	+2800	2119	+2800	2260
1.6 -Sink	+2800	+2800	+2800	+2800	+2800	+2800
Raw coal	2278	2080	2325	2145	2385	2300
	Float-Sink Size 14 Mesh x 0					
Float-1.3	2380	2110	2495	2265	2535	2630
1.3 -1.4	2200	1880	2283	2140	2375	2275
1.4 -1.6	2465	2380	2538	2435	2582	2530
1.6 -Sink	2670	2560	+2800	+2800	+2800	+2800

Oxi.(Oxidizing atmosphere)
Red.(Reducing atmosphere)
x. cone condition not recognizable

Table 5-25 Ash fusion initial deformation temperature exponetial to Ratio K in the case of Healy coal

Product	Initial deformation temperature Observed	Predicted	Residual
Float-Sink Size 1-1/2 inches x 100 Mesh (Oxidizing atmosphere)			
Float-1.3	2130	2111	19
1.3 -1.4	2230	2218	12
1.4 -1.6	2330	2761	-31
1.6 -Sink	2512	2483	28
R-Squared = 0.97	prediction = $1999 \times e^{0.06k}$		
(reducing atmosphere)			
Float-1.3	1910	1930	-20
1.3 -1.4	2154	2100	54
1.4 -1.6	2287	2340	53
1.6 -Sink	2575	2553	22
R-squared =0.97	prediction = $1736 \times e^{0.11k}$		

Reproduced with permission of the copyright owner. Further reproduction prohibited without permission.

Table 5-26 Ash fusion initial deformation temperature exponetial to Ratio K in the case of Chignik coal

Product	Initial deformation temperature Observed	Predicted	Residual
Float-Sink Size 14 Mesh x 0 (Oxidizing atmosphere)			
Float-1.3	2020	2000	20
1.3 -1.4	2230	2255	-25
1.4 -1.6	2400	2458	-58
1.6 -Sink	2620	2553	67
R-Squared = 0.96	prediction = 1731 x $e^{0.21k}$		
(Reducing atmosphere)			
Float-1.3	1990	1977	13
1.3 -1.4	2231	2242	-11
1.4 -1.6	2395	2455	-60
1.6 -Sink	2614	2554	60
R-squared = 0.97	prediction = 1698 x $e^{0.22k}$		

Reproduced with permission of the copyright owner. Further reproduction prohibited without permission.

Table 5-27 Ash fusion initial deformation temperature exponetial to Ratio K in the case of Johnson Creek coal

Product	Initial deformation temperature Observed	Predicted	Residual
Float-Sink Size 1-1/2 inches x 100 Mesh (Oxidizing atmosphere)			
Float-1.3	2147	2117	30
1.3 -1.4	2190	2214	-24
1.4 -1.6	2307	2349	-42
1.6 -Sink	2520	2482	38
R-Squared = 0.94	prediction = $1821 \times e^{0.11k}$		
(Reducing atmosphere)			
Float-1.3	1945	1942	3
1.3 -1.4	2016	2011	5
1.4 -1.6	2080	2108	-28
1.6 -Sink	2222	2203	19
R-squared =0.97	prediction = $1719 \times e^{0.09k}$		

Reproduced with permission of the copyright owner. Further reproduction prohibited without permission.

has an accuracy of about less than 64°F. A universial regression across the limit of all samples yielded 200°F accuracy for multiple linear regression.

The correlation measured from ratio K gives better accuracy if different sizes are treated separately. The correlation measured from the multiple linear regression for different sizes of raw coal shows the prediction closer to the observed value (Table 5-28 to 5-30). The ratio K also reflects the size liberation effect for certain elements revealed by ash fusion behavior. Table 5-31 gives the K value for various densimetric fractions.

V) Trace elements

Tables 5-32 to 5-37 give concentration of trace elements in the ash of various densimetric fractions. Concentrations of Cu, Cd, and Cr increases as separation specific gravity increased only in the case of Healy coal. In the other cases, all elements were more concentrated in the light fractions. Those having high concentrations in the light fractions indicate that they are of more "inherent" or organic origin than of "extraneous". Concentration of Co in the light fractions in all cases is high. For those organic associated elements, they are more related to the

Reproduced with permission of the copyright owner. Further reproduction prohibited without permission.

Table5-28 Comparison of observed and predicted initial defromation temperature for Healy coal

Product	Initial deformation temperature (Reducing atmosphere) Observed	Predicted	Residual
	Float-Sink Size 1-1/2 inches x 100 Mesh		
Float-1.3	2130	2145	-15
1.3 -1.4	2230	2120	
1.4 -1.6	2330	2345	-15
1.6 -Sink	2512	2509	3
Raw coal	2115	2175	-60
	Float-Sink Size 14 Mesh x 0		
Float-1.3	2072	2056	16
1.3 -1.4	2080	2133	-53
1.4 -1.6	2130	2118	12
1.6 -Sink	2402	2371	31

R-squared =0.92

Standard Error of Estimate =71

prediction = $-3171.0+59.3SiO_2+64.9Al_2O_3+6.8Fe_2O_3-63.3MgO+80.1CaO$

Reproduced with permission of the copyright owner. Further reproduction prohibited without permission.

Table 5-29 Comparison of observed and predicted initial deformation temperature for Chignik coal

Product	Initial deformation temperature (Redicing atmosphere) Observed	Predicted	Residual
Float-Sink Size 1-1/2 inches x 100 Mesh			
Float-1.3	2034	2030	4
1.3 -1.4	2270	2284	-14
1.4 -1.6	2520	2512	7
1.6 -Sink	2630	2617	12
Raw coal	2580	2579	1
Float-Sink Size 14 Mesh x 0			
Float-1.3	1990	1989	1
1.3 -1.4	2231	2234	-3
1.4 -1.6	2395	2387	8
1.6 -Sink	2614	2631	-17

R-squared =0.99

Standard Error of Estimate =16

prediction = $1348.4+39.4SiO_2-34.0Al_2O_3-16.9Fe_2O_3+8.2MgO+55.8CaO$

Reproduced with permission of the copyright owner. Further reproduction prohibited without permission.

Table 5-30 Comparison of observed and predicted initial deformation temperature for Johnson Creek coal

Product	Initial deformation temperature (Reducing atmosphere) Observed	Predicted	Residual
	Float-Sink Size 1-1/2 inches x 100 Mesh		
Float-1.3	1945	1919	26
1.3 -1.4	2016	1967	49
1.4 -1.6	2080	2064	16
1.6 -Sink	2222	2235	-13
Raw coal	1948	2012	-64
	Float-Sink Size 14 Mesh x 0		
Float-1.3	1935	1978	-43
1.3 -1.4	2050	2007	42
1.4 -1.6	1985	2040	-55
1.6 -Sink	2220	2177	43

R-squared =0.84

Standard Error of Estimate =73

prediction = $7599.4-51.3SiO_2-92.6Al_2O_3-64.1FeO_2O_3+350.4MgO$ $-130.0CaO$

Reproduced with permission of the copyright owner. Further reproduction prohibited without permission.

Table-5-31 Ratio $K=SiO_2/Al_2O_3$ from the ash of each sample

Product	Healy	Chignik	Cape Beaufort	Evan Jones	Johnsons Creek	Beluga
			Float-Sink Size 1-1/2 inches x 100 Mesh			
Float-1.3	0.96	0.93	0.00	1.83	1.41	0.80
1.3 -1.4	1.73	1.48	1.68	1.66	1.83	1.43
1.4 -1.6	2.71	1.69	2.00	1.96	2.39	1.60
1.6 -Sink	3.50	1.84	2.71	2.13	2.90	1.70
Raw coal	3.12	1.82	2.52	2.07	2.08	1.45
			Float-Sink Size 14 Mesh x 0			
FLOAT-1.3	1.61	0.69	0.00	1.02	1.25	0.98
1.3 -1.4	1.91	1.26	1.68	1.47	1.77	1.42
1.4 -1.6	2.37	1.67	1.92	1.97	2.24	1.59
1.6 -Sink	4.03	1.85	2.65	2.09	2.64	1.87

Reproduced with permission of the copyright owner. Further reproduction prohibited without permission.

Reproduced with permission of the copyright owner. Further reproduction prohibited without permission.

Table-5-32

Distribution of trace element in the ash of washability products from the No.3 Bed Coal Sample (UA-130) Usibelli Coal Mine, Healy, Alaska

Raw Coal Bed Moisture = 24.54

	Actual Product%		concentration/ppm					
Product	Wt	Ash	Cu	Zn	Co	Ni	Cd	Cr
			Float-Sink Size 1-1/2 inches x 100 Mesh					
Float-1.3	16.09	4.63	78	90	91	265	3	62
1.3 -1.4	69.12	6.81	150	76	67	210	5	119
1.4 -1.6	6.62	13.44	234	76	41	125	6	134
1.6 -Sink	8.17	68.75	292	61	0	15	6	151
Raw coal			211	139	45	137	7	80
			Float-Sink Size 14 Mesh x 0					
Float-1.3	15.31	4.60	141	166	107	296	4	89
1.3 -1.4	68.45	9.12	166	109	61	191	4	68
1.4 -1.6	9.06	17.87	236	124	25	88	6	95
1.6 -Sink	7.18	70.92	242	332	27	68	7	117

All results are on a Moisture Free Basis.

Reproduced with permission of the copyright owner. Further reproduction prohibited without permission.

Table-5-33

Distribution of trace element in the ash of washability products from an Uncorrelated Bed Coal Sample (UA-136) Chignik Mine, Chignik, Alaska

Raw Coal Bed Moisture = 6.66

	Actual product%		Concentration/ppm					
product	wt	Ash	Cu	Zn	Co	Ni	Cd	Cr
			Float-Sink Size 1-1/2 inches x 100 Mesh					
Float-1.3	5.76	4.06	140	225	59	68	6	208
1.3 -1.4	29.80	7.65	87	171	27	40	6	114
1.4 -1.6	14.69	20.49	63	111	14	24	5	67
1.6 -Sink	49.75	59.53	55	70	8	24	5	56
Raw coal			64	82	12	25	4	49
			Float-Sink Size 14 Mesh x 0					
Float-1.3	4.19	2.75	137	207	97	98	5	139
1.3 -1.4	31.34	8.00	175	478	33	74	2	234
1.4 -1.6	16.00	20.69	100	188	13	29	6	80
1.6 -Sink	48.47	59.34	50	145	9	22	4	43

All results are on a Moisture Free Basis.

Reproduced with permission of the copyright owner. Further reproduction prohibited without permission.

Table-5-34

Distribution of trace element in the ash of washability products from the No. 7 Bed Coal Sample (UA-139). Cape Beaufort, Alaska

Raw Coal Bed Moisture = 11.25

	Actual Product%	concentration/ppm					
Product	Wt	Ash	Cu	Zn	Co	Ni	Cd	Cr
		Float-Sink Size 1-1/2 inches x 100 Mesh						
Float-1.3	0.00	0.00	0	0	0	0	0	0
1.3 -1.4	11.55	5.32	54	164	32	40	4	24
1.4 -1.6	64.65	12.20	41	196	7	20	4	12
1.6 -Sink	23.80	60.01	4	125	0	8	4	0
		Float-Sink Size 14 Mesh x 0						
Float-1.3	0.00	0.00	0	0	0	0	0	0
1.3 -1.4	8.65	4.90	115	185	33	48	4	33
1.4 -1.6	51.74	9.73	53	123	8	21	4	16
1.6 -Sink	39.61	50.42	20	149	2	13	7	1

All results are on a Moisture Free Basis.

Table-5-35

Distribution of trace element in the Ash of washability products from the No. 5 Bed Coal Sample (UA-147) Evan Jones Mine, Matanuska, Alaska

Raw Coal Bed Moisture = 4.82

	Actual product%		concentration/ppm					
Product	Wt	Aqh	Cu	Zn	Co	Ni	Cd	Cr
		Float-Sink Size 1-1/2 inches x 100 Mesh						
Float-1.3	11.70	2.92	177	747	225	680	9	292
1.3 -1.4	22.01	10.09	183	453	75	237	9	292
1.4 -1.6	22.45	24.12	165	598	31	118	9	212
1.6 -Sink	43.84	61.04	93	273	13	66	9	77
Raw coal			103	886	12	70	8	143
		Float-Sink Size 14 Mesh x 0						
Float-1.3	4.18	2.96	219	409	219	760	19	295
1.3 -1.4	28.52	5.63	210	329	83	333	10	219
1.4 -1.6	21.80	22.60	179	333	30	141	13	136
1.6 -Sink	45.50	55.16	93	728	12	67	9	114

All results are on a Moisture Free Basis.

Reproduced with permission of the copyright owner. Further reproduction prohibited without permission.

Reproduced with permission of the copyright owner. Further reproduction prohibited without permission.

Table-5-36

Distribution of trace element in the Ash of washability products from an Uncorrelated Bed Coal Sample (UA-149) Johnson Creek, Yentna Field, Alaska

Raw Coal Bed Moisture = 25.34

	Actual Product%		concentration/ppm					
Product	Wt	Ash	Cu	Zn	Co	Ni	Cd	Cr
		Float-Sink Size 1-1/2 inches x 100 Mesh						
Float-1.3	31.97	5.24	218	440	49	169	8	167
1.3 -1.4	47.26	10.78	245	607	28	132	8	115
1.4 -1.6	14.30	28.77	167	240	9	80	11	228
1.6 -Sink	6.47	64.21	67	207	7	62	11	158
Raw coal			158	290	22	100	8	192
		Float-Sink Size 14 Mesh x 0						
Float-1.3	26.15	4.87	232	240	63	193	12	119
1.3 -1.4	44.91	9.01	230	187	38	144	7	91
1.4 -1.6	16.87	23.78	135	141	15	72	7	79
1.6 -Sink	12.07	39.74	97	232	8	65	8	126

All results are on a Moisture Free Basis.

Reproduced with permission of the copyright owner. Further reproduction prohibited without permission.

Table-5-37

Distribution of trace element in the Ash of washability products from Green Bed Coal Sample (UA-152) Long Ridge Mine, Beluga Field, Alaska

Raw Coal Bed Moisture = 27.59

	Actual Product%	concentration/ppm					
Product	Wt	Ash	Cu	Zn	Co	Ni	Cd	Cr
		Float-Sink Size 1-1/2 inches x 100 Mesh						
Float-1.3	64.10	3.55	128	340	39	122	13	89
1.3 -1.4	31.39	7.16	145	242	23	76	10	92
1.4 -1.6	2.97	22.06	65	195	2	41	3	52
1.6 -Sink	1.54	64.69	35	210	0	24	5	0
Raw coal			99	284	21	78	11	79
		Float-Sink Size 14 Mesh x 0						
Float-1.3	51.70	3.80	134	354	33	117	12	49
1.3 -1.4	39.22	7.39	260	196	40	38	7	91
1.4 -1.6	16.87	23.78	135	141	15	72	7	79
1.6 -Sink	12.07	24.00	211	144	0	25	8	13

All results are on a Moisture Free Basis.

macerals liberation than any other factors. Statistical regression of separation specific gravity related to element distribution in the fractions is also of concern. In general, they all have good agreement with a parabolic relationship. More data to confirm the regression are needed.

Reproduced with permission of the copyright owner. Further reproduction prohibited without permission.

CONCLUSIONS AND RECOMMENDATIONS

Conclusions

The conventional approach of washability studies of coal that evaluates the product quality in terms of ash and heating value can not satisfy the demands for such wide uses as power genernation, coke making and liquefaction. The chemical components of ash from each densimetric fraction as well as petrology of samples are of special concern because of their relation to system performance in end use. The study results lead to the following conclusions:

A) The maceral groups and microlithotypes analysis is an effective method for quality control of macerals concentration by washability process. Liptites were absent in all six coals studied, durite was found only in trace quantities and in a few cases, vitrite concentration was higher in lower density fractions and inertite was concentrated in higher density fractions as expected. Clarite is concentrated in lower density fractions except in cases where it is associated with inorganic material. Vitrinertite is generally concentrated in the intermediate density fractions for coarse samples and is concentrated in higher density fraction in finer material. The studies also show

Reproduced with permission of the copyright owner. Further reproduction prohibited without permission.

macerals liberation due to crushing and prove that possibilities of petrographic beneficiation of samples in certain cases.

B) The trend of concentration of major elements in the ash is related to washability process and allows quality control of ash composition for different utilization systems, even though, the separation processes of minerals from coal itself is not fully established. Major oxides such as SiO_2, Al_2O_3, and K_2O are present as inorganic minerals and are thus concentrated in the higher density fractions. MgO and CaO are present as organic chelates and are thus concentrated in the lower density fractions. Fe_2O_3 and MnO are concentrated in the lower density fractions in most cases. P_2O_5 and SO_3 are associated with organic material and are therefore concentrated in the lower density fractions.

C) A knowledge of concentration of minerals in different densimetric fractions shows the possibility of separation from coal, which provides the possibility of blending washability products to dilute certain chemical constituents in the ash to satisfy specifications for different purposes. Quartz and kaolinite are concentrated in the higher density fractions in all cases from their densimetric fractions study. Due to the small amount of carbonates in the coal, it is hard to have precise conclusions

Reproduced with permission of the copyright owner. Further reproduction prohibited without permission.

from their densimetric fractions study.

The ash fusibility can be predicted from ash composition and therefore provides a direct means of relating coal washability to combustion problems.

E) The trend of trace element concentration appears to be related to major oxides and macerals distribution in the densimetric fractions and is a function of its source and origin.

Recommendations

In order to have exact quality control of coal to be used in various utilization systems, washability studies will need to more fully examine the products and the following further studies are recommended:

1. Examination of associations between chemical elements and macerals.
2. Improvements in the accuracy of mineralogic analysis from LTA, such as improved Fourier-Transform Infrared Analyses.
3. The development of quantitative analytical methods for estimation of "other clays".

Reproduced with permission of the copyright owner. Further reproduction prohibited without permission.

GLOSSARY

Dilatometer--- The dilatometer test for coal measures change in the volume and the fusing together of the plastic particles that occur during heating up and are important to the formation of coke.

Macerals--- The term maceral decribes both the shape and the nature of the microscopically recognizable constituents of the coal.

Microlithotypes--- The macerals of coal, particularly those of the exinite group as well as micrinite and macrinite, rarely occur by themselves; they are more usually associated with macerals of the same or of the two other maceral groups. Such association are termed "microlithotypes".

Swelling index--- The swelling of coking properties of coal at a prescribed rate to 1508^{o} F and measuring the size or Free Swelling Index (FSI) of the coke bottom formed (ASTM 0720). Like fluidity, the FSI is used as an indicator of the coking quality of coal.

Slag tap furnaces--- Pulverized coal fired units may be classified broadly into two types according to whether their furnaces are designed for removal of ash in dry or molten form. The

Reproduced with permission of the copyright owner. Further reproduction prohibited without permission.

molten ash furnaces are normally called "slag tap" or "wet bottom" furnaces.

Washability--- A washability analysis is an evaluation of the physical properties of a coal that determine its amenability to improvements in quality by gravity separation methods. It includes stage crushing to show potential release of impurities, and specific gravity fractionation to show the quality and quantity of the cleaned product. A washability analysis is made by fractionating the coal sample at preselected, carefully controlled specific gravity. This is termed float-sink analysis or specific gravity separation.

Reproduced with permission of the copyright owner. Further reproduction prohibited without permission.

REFERENCES

Barnes. F.F., Geology and Coal Resources of the Beluga-Yentna Region Alaska: U.S. Geol. Survey Bull. 1202-C, 54p, 1966.

Barnes, F.F. and Paynes, Thomas G., The Wishbon Hill District, Matanuska Coal Field, Alaska: U.S. Geol. Survey Bull. 1016,88p, 1956.

Benedict L.G., and Thompson R.R., presented at the Annual Meeting, Northeast Section, Geological Society of America, Allentown Pa., March 22, 1973.

Benedict L.G., Thompson R.R., and Wenger R.C., Blast Furn. Steel Plant 1968.

Blumer, J.W., Review of Mobil Coal Leases---Yentna Region, Alaska, Proceedings of Coal Conf., Focus on Alaska's coal '80, Mineral Industry Research Laboratory, Report No. 50, University of Ak, 9. 122-126, 1980.

Brown H.R., Taylor G.H., and Cook A.C., "Prediction of Coke Strength from the Rank and Petrographic Composition of Australian Coals." Fuel, 43(1), 43-54, 1964. Cavallaro J.A., Gibbon G.A. and Devrbrouck A.W., "A Washability and Analytical Evaluation of Potential Pollution from Trace elements in Coal" DOE/PB-280 759, 1978.

Cook A.C., and Edwards G.E., Fuel, 50, 41-52, 1970.

Reproduced with permission of the copyright owner. Further reproduction prohibited without permission.

Cook A.C., and Wilson R.G., Australas. Inst. Min. Metall. Proc., No. 232, 27-39, 1969. Corey R.C. et al., "Occurrence and Determination of Germanium in Coal Ash from Power Plants" U.S. Bur. Mines Bull. No. 575, 68pp, 1959.

Crossley H.E., and Marskell W.G., Proc. Joint Conf. on Combustion, Inst. Mech. Engrs. London, 19p. 72-5, 1955.

Denton, Steve W., "Geology and Coal Resources of the Lower Lignite Creek Area", Proceedings of Conf., Focus on Alaska's coal '80, Mineral Industry Research Laboratory, Report No. 50, University of Ak, pp 138-143, 1980.

Given P.H., Cronauer W.S., Lovell H.L., David A., and Biswas B., Fuel, 54, 34, 1975 & 40, 1975.

Goldschmidt V.M., "Occurrence of Rare Elements in Coal Ashes." Progress in Coal Science. Interscience, New York. 238-247, 1950.

Gorin Everett, "Characterization of Coal Ash and Its Influence on Coal Conversion Process." Paper presented at Gordon Conf. Coal Science, New Hampton, N.H., July 24, 1975.

Gorin Everett, "The Effect of Coal-derived Minerals on the Activity of Hydrogenation Catalysts." paper presented at Gordon Conf. Coal Science, New Hampton, N.H., July 2, 1969.

Gorin Everett, Kulik C.J., and Lebowitz H.E., Ind. Eng. Chem.

Reproduced with permission of the copyright owner. Further reproduction prohibited without permission.

Process Des. Dev., 16(1), 102, 1977.

Gray R.J., J. Inst. Fuel, 37 234-242, 1964.

Gronhovd G.H., Harak W.E., Kube W.R., and Oppelt W.H., "Design and Initial Operation of a Slagging , Fixed Bed, Pressure Gasification Pilot Plant." U.S. Bur. Mines Rep. Invest. No. 6085, 1962, 50pp.

Gumz W., Combustion, 27, No. 10, 47-54, No. 11, 53-4, 1956.

Hatch J.R., Gluskoter H.J., and Lindahl P.C., "Sphalerite in Coals from the Illinois Basin." Econ. Geol., 71, 613-624, 1976.

Headlee A.J.W., and Hunter R.G., "Germanium in Coal of West Virginia" West Virginia Geol. Econ. Survey Rept. Invest, 8, 1-15, 1951. Morgantown.

Hoy H.R., Roberts A.G., and Wilkins D.M., "Behavior of Mineral Matter in Slagging Gasification Processes." J. Inst. Gas Eng., 5, 444-469, June 1965.

Kang C.C., and Johanson E.S., Prepr., Am. Chem. Soc., Div. Fuel Chem., 21(5), 32, 1976.

Kovach S.M., and Bennett J., Prepr., Am. Chem. Sco., Div. Fuel Chem., 20(1), 143, 1975.

Krause H.H., Levy A., and Reid W.T., "Radioactive Sulfur Oxide Studies of External Corrosion Reactions on Surfaces," ASME

Reproduced with permission of the copyright owner. Further reproduction prohibited without permission.

paper No.68-WA/CD-2, 1968.

Krejci-Graf K., "Trace Metals in Sediments, Oils, and Allied Substances." The Encyclopedia of Geochemistry and Environmental Sciences. Ed. R.W. Fairbridge. Van Nostrand Reinhold Com. New York, 1201-1209, 1972.

Kroger, C., Kuthe F. & Gondermann H., "Die physikalischen und chemischen Eigenschaften der steinkohlenmacerale. IV. Swelling-index, Dilatometertest.-Brennst.-Chemie 38, 147-151, 1957.

Mukherjee D.K., and Choudhury P.B., Fuel, 55, 4, 1976.

Natusch D.F.S., Wallace J.R., and Evans C.A., Jr., "Toxic Trace Elements: Preferential Concentration in Respirable Particles." Science, 183, 202-204, 1977.

Nelson J.B., BCURA Bull., 17, 41-55, 1953.

O'Gorman J.V., and Walker Jr., P.L., "Mineral Matter and Trace Elements in U.S. Coals." Office of Coal Research, R&D. Report No. 61, Interim Report No. 2, 1972.

Rao, P.D. and Wolff, E.N., "Characterization and Evaluation of Washability of Alaskan Coals." Final Technical Report for Phase III, DOE/ET/13350-T6, 1982a.

Rao P.D. and Wolff, E.N., "Characterization and Wolff, Evaluation of Washability of Alaskan Coal." Final Technical Report for

Reproduced with permission of the copyright owner. Further reproduction prohibited without permission.

Phase IV, DOE/ET/13350-T5, 1982b.

Rao, P.D. and Wolff, E.N., "Characterization and Evaluation of Washability of Alaskan Coals." U.S. DOE Final Report for Phase II, (DOE/ET/!/13350/-T2), 1980.

Rao,P.D. and Wolff, E.N., "Characterization and Evaluation of Washability of Alaskan Coals; U.S. DOE Final Technical Report for phase I, (NTIS FE-78-8969-1), 1979.

Rao C.P., and Gluskoter H.J., Occurrence and Distribution of Minerals in Illinois Coals, Illinois Geol. Survey Circ., 476, 1973.

Reid W.T., External Corrosion and Deposits: Boilers and Gas Turbines. Elsevier Publishing Company, New York, 1971, p.55.

Sage W.L., and Mcilroy J.B., "Relationship of Coal-ash Viscosity to Chemical Composition." Trans. ASME, J.Eng. Power, Serr. A, 62, 145-155 1960.

Schapiro N., and Gray R.J., Inst. Fuel, 234-242, June, 1964.

Schapiro N., and Gray R.J., Blast Furn. Steel Plant, 273-280, April 1963.

Schapiro, N., and Gray R. J., and Eusner G. R., "Resent Development in Coal Petrography." Blast Furnace, Coke Oven and Raw Materials Committee, proc. 20, 89-112, 1961.

Snyman C. P., "Die Petrographie sudafrikanischer Gondwanakohlen.

Reproduced with permission of the copyright owner. Further reproduction prohibited without permission.

Ein Vergleich zwischen Gondwana- und Euramerischen KOhlen." Diss. Univ. Bonn, 135pp, 1961.

Stach, E., Mackowsky M.Th., Teichmuller M., Taylor G.H., Chandra D., Teichmuller R., Stach's Textbook of Coal Petrology, 3rd edi. 1982.

Stach, E., Mackowsky M.Th., Teichmuller M., Taylor G.H., Chandra D., Teichmuller R., Stach's Textbook of Coal Petrology, 1st&2rd edi. 1971,1975.

Thompson R.R., Bethlehem Steel Corp. Personal Communication of unpublished work,1977.

Thompson R.R., and Benedict L.G., "Vitrinitic Reflectance as an Indicator of Coal Metamorphism for Coke-making." Geol. Soc. America Spec. paper No. 153, pp 95-108, 1974.

Thompson R.R., Mantione A,F., and Aikman R.P., presented at Pittsburgh Regional Technical Meeting of AISI, Nov. 12, 1970.

Van Hook R.I., and Shults' W.D., U.S. Energy & Research & Development Administration, Effect of Trace Element Contaminants from Coal Combustion, ERDA-77-64, Proceedings of Work-shop, Eds., Knoxville, Tenn., 1977.

Warfield R.S., and Boley Charles C., Sampling and Coking Studies of Several Coal Beds in the Kokolik River, Kukpowruk River

Reproduced with permission of the copyright owner. Further reproduction prohibited without permission.

and Cape Beaufort Areas of the Artic Northwestern Alaska, U.S. Bureau of Mines, RI 7321, 58p, 1969.

Watt J.D., and Fereday F., "The Flow Properties of Slags Formed from the Ashes of British Coals. Part 1. Viscosity of Homogeneous Liquid Slags in Relation to Slag Composition." J. Inst. Fuel, 42, 99-103, March 1969.

Yavorsky P.M., and Gorin E., "Utilization of Radioactive Isotopes in Coal Process Research, unclassified report to U.S. Atomic Energy Commission No. NYC-9852, under contract No. AT(30-1)-2350, May 1962.

Reproduced with permission of the copyright owner. Further reproduction prohibited without permission.